# TERRAIN MODELING AND ATMOSPHERIC TURBULENT FLOW SOLUTIONS BASED ON METEOROLOGICAL WEATHER FORECAST DATA

A THESIS SUBMITTED TO
THE GRADUATE SCHOOL OF NATURAL AND APPLIED SCIENCES
OF
MIDDLE EAST TECHNICAL UNIVERSITY

BY

ENGIN LEBLEBICI

IN PARTIAL FULFILLMENT OF THE REQUIREMENTS
FOR
THE DEGREE OF MASTER OF SCIENCE
IN
AEROSPACE ENGINEERING

JANUARY 2012

Approval of the thesis:

**TERRAIN MODELING AND ATMOSPHERIC TURBULENT FLOW SOLUTIONS BASED ON METEOROLOGICAL WEATHER FORECAST DATA**

submitted by **ENGIN LEBLEBICI** in partial fulfillment of the requirements for the degree of
**Master of Science in Aerospace Engineering Department, Middle East Technical University** by,

Prof. Dr. Canan Özgen
Dean, Graduate School of **Natural and Applied Sciences** _____

Prof. Dr. Ozan Tekinalp
Head of Department, **Aerospace Engineering** _____

Prof. Dr. İsmail Hakkı Tuncer
Supervisor, **Aerospace Engineering Department, METU** _____

**Examining Committee Members:**

Prof. Dr. Cevdet Çelenligil
Aerospace Engineering, METU _____

Prof. Dr. İsmail Hakkı Tuncer
Aerospace Engineering, METU _____

Assoc. Prof. D. Funda Kurtuluş
Aerospace Department, METU _____

Assist. Prof. Dr. Dr. Oğuz Uzol
Aerospace Engineering, METU _____

Assist. Prof. Dr. Mustafa Kaya
Aeronautical Sciences, THK University _____

**Date:** _____

**I hereby declare that all information in this document has been obtained and presented in accordance with academic rules and ethical conduct. I also declare that, as required by these rules and conduct, I have fully cited and referenced all material and results that are not original to this work.**

Name, Last Name: ENGIN LEBLEBICI

Signature :

# ABSTRACT

TERRAIN MODELING AND ATMOSPHERIC TURBULENT FLOW SOLUTIONS BASED ON METEOROLOGICAL WEATHER FORECAST DATA

Leblebici, Engin

M.S., Department of Aerospace Engineering

Supervisor : Prof. Dr. İsmail Hakkı Tuncer

January 2012, 58 pages

In this study, atmospheric and turbulent flow solutions are obtained using meteorological flowfield and topographical terrain data in high resolution. The terrain topology of interest, which may be obtained in various resolution levels, is accurately modeled using structured or unstructured grids depending on whether high-rise building models are present or not.

Meteorological weather prediction software MM5, is used to provide accurate and unsteady boundary conditions for the solution domain. Unsteady turbulent flow solutions are carried out via FLUENT with the help of several User Defined Functions developed.

Unsteady flow solutions over topographical terrain of METU campus are computed with 25m x 25m x 15m resolution using structured grids. These FLUENT solutions are compared with the MM5 solutions. Also, the accuracy of the boundary layer velocity profiles is assessed. Finally, effects of surface roughness model extracted from MM5 for the region of interest is investigated.

In addition, unsteady flow solutions over METU campus are repeated in presence of

high-rise building models using unstructured grids with resolution varying from 5 meters around buildings to 80 meters further away.
The study shows that unsteady, turbulent flow solutions can be accurately obtained using low resolution atmospheric weather prediction models and high resolution Navier-Stokes solutions over topographical terrains.

Keywords: Renewable Energy, Wind Turbine, Meteorological weather prediction software, Navier-Stokes Solver

# ÖZ

ARAZİ MODELLEME VE METEOROLOJİK VERİLERE DAYALI
ATMOSFERİK AKIŞ ÇÖZÜMLERİ

Leblebici, Engin
Yüksek Lisans, Havacılık Mühendisliğ Bölümü
Tez Yöneticisi : Prof. Dr. İsmail Hakkı Tuncer

Ocak 2012, 58 sayfa

Bu çalışmada atmosferik ve türbülanslı akım çözümleri meteorolojik akış alanı ve topografik arazi verileri kullanılarak yüksek çözünürlükte elde edilmiştir. Farklı çözünürlüklerde elde edilmiş olan ilgili arazinin topolojisi yüksek bina modellerinin olup olmadığına göre yapılı veya yapısız çözüm ağlarıyla hassas bir şekilde modellenmiştir.
Meteorolojik hava tahmin yazılımı MM5, çözüm alanı için hassas ve zamana bağlı sınır koşullarının eldesi için kullanılmıştır. Zamana bağlı türbülanslı akış çözümleri, FLUENT ile geliştirilen birkaç Kullanıcı Tanımlı Fonksiyon yardımıyla gerçekleştirilmiştir. Zamana bağlı akış çözümleri ODTÜ yerleşkesinin topografik arazisi üzerinde 25m x 25m x 15m çözünürlükte yapılı çözüm ağları kullanılarak hesaplanmıştır. Bu FLUENT çözümleri MM5 çözümleriyle karşılaştırılmıştır. Ayrıca sınır tabaka hız profilleri doğruluğu değerlendirilmiştir. Son olarak MM5' dan alınan yüzey pürüzlülük modelinin etkileri incelenmiştir.
Ek olarak ODTÜ kampüsü üzerinde zamana bağlı akış çözümleri yüksek katlı bina modelleri varlığında, bina çevresinde 5 metreden uzaklara doğru 80 metreye varan bir çözünürlükte yapısız çözüm ağları kullanılarak tekrarlanmıştır.

Çalışma, zamana bağlı türbülanslı akış çözümlerinin, düşük çözünürlüklü atmosferik tahmin bilgileri ve yüksek çözünürlüklü topografik araziler üzerinde Navier-Stokes çözümleri kullanılarak doğru bir şekilde elde edilebileceğini göstermektedir.

Anahtar Kelimeler: Yenilenebilir Enerji, Rüzgar Türbinleri, Meteorolojik Hava Tahmin Programları, Navier-Stokes Çözücü

# ACKNOWLEDGMENTS

I would like to thank to Prof. Dr. İsmail Hakkı Tuncer for teaching me to learn throughout my thesis. His guidance helped me in every step of this study.

I would like to thank Gökhan Ahmet for providing the MM5 data which is invaluable for this study, his constructive criticisms and his support.

Finally, I would like to express my sincere thanks to my family for their thrust and understanding.

# TABLE OF CONTENTS

ABSTRACT . . . . . iv

ÖZ . . . . . vi

ACKNOWLEDGMENTS . . . . . viii

TABLE OF CONTENTS . . . . . ix

LIST OF TABLES . . . . . xi

LIST OF FIGURES . . . . . xii

CHAPTERS

1 INTRODUCTION AND LITERATURE REVIEW . . . . . 1

2 METHODOLOGY . . . . . 8

2.1 MM5 SOLUTIONS . . . . . 9

2.2 DISCRETIZATION OF THE SOLUTION DOMAIN . . . . . 12

2.2.1 DISCRETIZATION OF SOLUTION DOMAIN OVER TOPOGRAPHICAL TERRAIN . . . . . 13

2.2.2 DISCRETIZATION OF SOLUTION DOMAIN OVER TOPOGRAPHICAL TERRAINS WITH HIGH-RISE BUILDING MODELS . . . . . 14

2.3 INITIAL AND BOUNDARY CONDITIONS . . . . . 16

2.3.1 INTERPOLATION OF MM5 SOLUTION AND OBTAINING VELOCITY PROFILES AT BOUNDARIES 18

2.3.2 SURFACE ROUGHNESS MODEL . . . . . 18

2.4 UNSTEADY FLUENT SOLUTIONS . . . . . 20

2.4.1 USER DEFINED FUNCTIONS (UDFS) FOR TIME AND SPATIALLY VARYING BOUNDARY CONDITIONS . . . . . 20

2.4.2 SOLVER SETTINGS AND ASSUMPTIONS . . . . 21

3 RESULTS AND DISCUSSION . . . . . 24
3.1 UNSTEADY ATMOSPHERIC FLOW SOLUTİONS OVER TOPOGRAPHICAL TERRAIN . . . . . 25
3.1.1 SIMULATION RESULTS FOR A DAY . . . . . 31
3.1.2 COMPARISON OF MM5 SOLUTIONS WITH FLUENT . . . . . 36
3.1.3 EFFECTS OF SURFACE ROUGHNESS MODEL . 43
3.2 UNSTEADY ATMOSPHERIC FLOW SOLUTIONS OVER TOPOGRAPHICAL TERRAIN WITH HIGH-RISE BUILDING MODELS . . . . . 48
4 CONCLUSION . . . . . 55
REFERENCES . . . . . 57

# LIST OF TABLES

TABLES

Table 2.1 USGS LANDUSE Categories . . . . . 19

# LIST OF FIGURES

FIGURES

Figure 1.1 Classification of weather systems and associated distance scales(re-illustrated)[20] . . . . . 4
Figure 1.2 Sigma levels(re-illustrated)[18] . . . . . 5
Figure 1.3 Contours of velocity magnitude with respect to altitude around Ankara shown on y (left) and z (right) plane cuts . . . . . 6
Figure 1.4 Wind speed vectors shown on a z-plane cut . . . . . 6

Figure 2.1 Basic flowchart for the computational method . . . . . 9
Figure 2.2 Flowchart for MM5 solutions . . . . . 10
Figure 2.3 Location of MM5 nodes around Ankara region . . . . . 11
Figure 2.4 All (right) and first 8 (left) sigma levels around METU campus . . . . 11
Figure 2.5 Flowchart for discretization of FLUENT solution domain . . . . . 12
Figure 2.6 Edges of the triangular surfaces for approximating the topography . . 14
Figure 2.7 Flowchart for obtaining time dependent boundary condition profiles . . 17
Figure 2.8 Flowchart for unsteady FLUENT Solutions . . . . . 20

Figure 3.1 Borders of MM5 and FLUENT solution domains . . . . . 26
Figure 3.2 Close-up view of FLUENT solution domain (left) and METU campus with MM5 nodes on the topography (right) . . . . . 26
Figure 3.3 MM5 nodes on the first eight sigma levels around METU campus (left) and FLUENT solution domain (right) . . . . . 26
Figure 3.4 Topography model for METU campus . . . . . 27
Figure 3.5 Surface meshes and meshed side edges for the FLUENT Solution Domain 28
Figure 3.6 Structured grid of the FLUENT solution domain . . . . . 28

Figure 3.7 Velocity magnitude contours of the FLUENT solution domain at the 0th hour of the simulation . . . . . 29

Figure 3.8 Velocity profiles for the velocity inlets at the 6th hour of the simulation 30

Figure 3.9 Velocity profiles for the velocity inlets at the 12th hour of the simulation 30

Figure 3.10 FLUENT solution domain with three terrain following surfaces 25, 50 and 100 meter above the ground . . . . . 31

Figure 3.11 Velocity magnitude contours with streamlines 25, 50 and 100m above the ground between 19:00 and 24:00 on 15.6.2010 . . . . . 32

Figure 3.12 Velocity magnitude contours with streamlines 25, 50 and 100m above the ground between 01:00 and 06:00 on 16.6.2010 . . . . . 33

Figure 3.13 Velocity magnitude contours with streamlines 25, 50 and 100m above the ground between 07:00 and 12:00 on 16.6.2010 . . . . . 34

Figure 3.14 Velocity magnitude contours with streamlines 25, 50 and 100m above the ground between 13:00 and 18:00 on 16.6.2010 . . . . . 35

Figure 3.15 Velocity magnitude contours of FLUENT and MM5 solutions 25m above the ground at the 1st, 6th, 12th and 24th hours of the simulation . 37

Figure 3.16 Velocity magnitude contours of FLUENT and MM5 solutions 50m above the ground at the 1st, 6th, 12th and 24th hours of the simulation . 38

Figure 3.17 Velocity magnitude contours of FLUENT and MM5 solutions 100m above the ground at the 1st, 6th, 12th and 24th hours of the simulation . 39

Figure 3.18 Velocity vectors of MM5 and FLUENT solutions and their differences at MM5 node Locations for the 1st hour of the simulation . . . . . 40

Figure 3.19 X (left) and Y (right) velocities in the middle of the domain for the 6th hour of the simulation . . . . . 41

Figure 3.20 Velocity magnitudes of FLUENT and MM5 solutions in the middle of the domain for the 1st hour of the simulation . . . . . 41

Figure 3.21 Velocity magnitudes of FLUENT and MM5 solutions in the middle of the domain for the 6th hour of the simulation . . . . . 42

Figure 3.22 Velocity magnitudes of FLUENT and MM5 solutions in the middle of the domain for the 12th hour of the simulation . . . . . 42

Figure 3.23 Roughness height profile for the topography of METU campus . . . . 43

Figure 3.24 Velocity magnitude contours and effects of roughness on velocity magnitude 25m above the ground at the 1st, 6th, 12th and 24th hours of the simulation . . . . . 44

Figure 3.25 Velocity magnitude contours and effects of roughness on velocity magnitude 50m above the ground at the 1st, 6th, 12th and 24th hours of the simulation . . . . . 45

Figure 3.26 Velocity magnitude contours and effects of roughness on velocity magnitude 100m above the ground at the 1st, 6th, 12th and 24th hours of the simulation . . . . . 46

Figure 3.27 Velocity magnitudes with and without roughness height profiles in the middle of the domain for the 1st hour of the simulation . . . . . 47

Figure 3.28 Velocity magnitudes with and without roughness height profiles in the middle of the domain for the 6th hour of the simulation . . . . . 48

Figure 3.29 Velocity magnitudes with and without roughness height profiles in the middle of the domain for the 12th hour of the simulation . . . . . 48

Figure 3.30 Flowfield with high-rise buildings . . . . . 49

Figure 3.31 Flowfield and meshes on the building models (left) and the surface mesh of the modified topography (right) . . . . . 49

Figure 3.32 Unstructured Mesh of the Flowfield with Building Models . . . . . 50

Figure 3.33 X plane cuts of the meshes around building models . . . . . 50

Figure 3.34 Close-up views of the meshes around building models . . . . . 51

Figure 3.35 FLUENT solution domain with z-plane cuts at 960, 985 and 1050 meters of altitudes . . . . . 51

Figure 3.36 Velocity Contours and streamlines at 960m altitude at the 1st, 6th, 12th and 24th hour of the Simulation and Close-up Views around MM and KKM Buildings . . . . . 52

Figure 3.37 Velocity Contours and streamlines at 985m altitude at the 1st, 6th, 12th and 24th hour of the Simulation and Close-up Views around MM and KKM Buildings . . . . . 53

Figure 3.38 Velocity Contours and streamlines at 1050m altitude at the 1st, 6th, 12th and 24th hour of the Simulation and Close-up Views around MM and KKM Buildings . . . . . 54

# CHAPTER 1

# INTRODUCTION AND LITERATURE REVIEW

Accurate predictions of unsteady rural and urban flow fields have a wide range of usage such as wind turbine site selection and pollution tracking, each of which are of recent research topics with several examples in literature[1],[2],[3],[4],[5].

Surrounded by mountains and where vast, high altitude valleys constitute most of the land, Turkey has very high wind energy potential. In recognition of this potential Elektrik İşleri Etüd İdaresi Genel Müdürlüğü (EİE) has developed Wind Energy Potential Atlas based on atmospheric observational data and simulations done by numerical weather prediction software.

As wind farms consisting of several wind turbines have a high initial investment cost, wind farm siting must be given a significant importance[6][4]. Low resolution wind energy potential atlases have the necessary statistical information for macro-siting of wind farms but lack the precision for the micro-siting. Therefore; high resolution, more accurate wind field information may be needed for micro-siting in order to improve the power output.

For micro-siting, widely used numerical models can be divided into 4 groups;

- Linearized Models
- RANS Reynolds Average modeling

- LES Large eddy simulation
- DNS Direct numerical simulation

Some of the mostly used commercial wind-farm design packages are WAsP, Windfarm, WindPRO, Openwind, MS-Micro/3, ShelCorr etc... All these software are developed in order to estimate the power production and increase the maximum energy output of the wind farm.

WAsP (Wind Atlas Analysis and Application Program) from Risø based on the concept of linearized flow models is the most popular model among the above[7]. It is a PC-program for horizontal and vertical extrapolation of wind data. The program contains a complete set of models to calculate the effects on the wind of sheltering obstacles, surface roughness changes and terrain height variations. The analysis part consists of a transformation of an observed wind climate (speed and direction distributions) to a wind atlas data set. The wind atlas data set can subsequently be applied for estimation of the wind climate and wind power potential, as well as for siting of specific wind turbines.[8]

- Developed initially for neutrally stable flow over hilly terrain
- Contains simple models for turbulence and surface roughness
- Best suited to more simple geometries
- Quick and accurate for mean wind flows
- Poorly predict flow separation and recirculation
- Limitations in more complex terrain regions due to the linearity of the equation set [9]

Also Bowen(2004)[10] in a Risø-R Report stated that Botta et al (1992)[11], Bowen and Saba (1995)[12], Reid (1995)[13] and Sempreviva et al (1986)[14] experience in the operation of commercial wind farms (Lindley et al., 1993[15]) has confirmed that

effects from the local complex terrain on the site characteristics of each turbine have a significant influence on the output (and perhaps even the viability) of a wind energy project.

F.J.Zajackowski et.al.[16] compares Numerical Weather Prediction Models (NWP) and Computational Fluid Dynamics (CFD) simulations very clear; NWP can take into account radiation, moist convection physics, land surface parameterizations, atmospheric boundary layer physics closures, and other physics. Wind flow features finer than 1 km are not captured by the turbulence physics of such models. CFD simulations, however, have proven useful at capturing the details of smaller scales in the flow around features such as buildings and fine scale topography.

Realtime flowfield data of a region also allows tracking of pollutants that move with the wind such as carbon monoxide, nitrogen oxides, sulphur oxides or nuclear particles. Accurate tracking of airborne pollutants using CFD methods is a current research topic.

Some of the major difficulties in the urban computational fluid dynamics applications are obtaining and utilizing unsteady boundary conditions, modeling of buildings and obtaining the topographical data for the surface of the flowfield (topography) to be analyzed.

For accurate flowfield predictions, terrain topology should be accurately modeled with vegetation and if present, buildings. Strangroom[5] states that complex landforms effect wind speed and several flow attributes relevant to wind speed significantly.

For obtaining the topography for the region to be analyzed, Yılmaz[1] used LIDAR which is an optical remote sensing technology that can measure the distance by illuminating the target using pulses from a laser to create CAD drawings for the geometry of the region and generated an unstructured mesh using GAMBIT software. Zheng[17]

used GIS (Geographical Information System) to model terrain and buildings coupled with Star-CD to simulate urban pollutant dispersion.

Most of the wind farm micro siting and pollution tracking studies assumes a steady velocity profile going in one direction for the boundary conditions but as the atmospheric flow is an irregular phenomenon, results of this assumption may be unrealistic in some cases.

Computational fluid dynamics applications, which use data from meteorological prediction software, exist. Laporte[18] stated that using the wind field information obtained from a mesoscale weather prediction software as initial conditions decreased the simulation time.

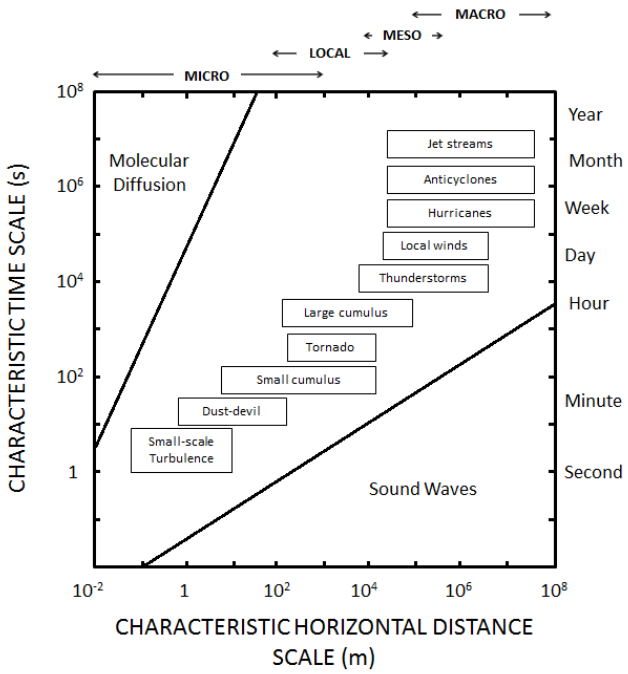


Figure 1.1: Classification of weather systems and associated distance scales(re-illustrated)[20]

The PSU/NCAR mesoscale model (known as MM5) is a limited-area, nonhydrostatic, terrain-following sigma-coordinate model designed to simulate or predict mesoscale

atmospheric circulation[19]. Mesoscale weather systems which includes phenomena such as local winds and thunder storms are defined in approximately from 2 km to 2000 km horizontal characteristic distance scale as shown in Figure 1.1.

This model gets the coordinates and altitude data for the flowfield to be analyzed from the United States Geographical Survey (USGS) and creates structured grid around the region to be analyzed. [19]. For vertical coordinates, MM5 uses terrain following sigma levels. The vertical coordinate, $\sigma$, is defined as:

$$\sigma = \frac{p - p_t}{p*} \tag{1.1}$$

and pressure perturbation $p*$ is simply

$$p* = p_s - p_t \tag{1.2}$$

where p is pressure, $p_s$ is surface pressure, and $p_t$ is the pressure at the top of the model as seen in Figure 1.2.

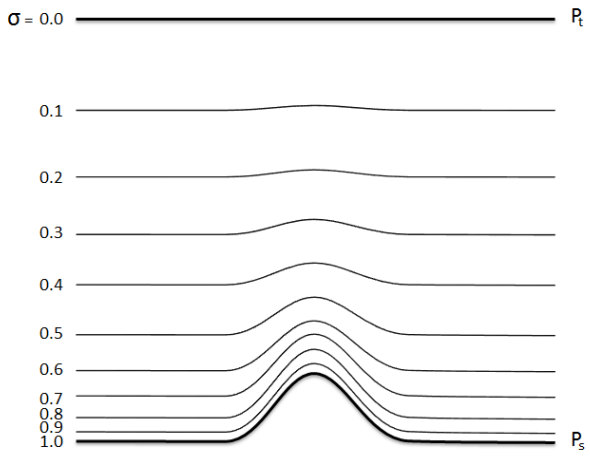


Figure 1.2: Sigma levels(re-illustrated)[18]

MM5 can be used to obtain the low resolution flowfield data for the determination of boundary and initial conditions. For instance, flow properties of a selected region

(Ankara) can be determined with a low resolution (2400 meter horizontal and maximum vertical resolution of 75 meter) (51x51x32) and it can be seen that wind speed is changes with altitude in Figure 1.3 and Figure 1.4.

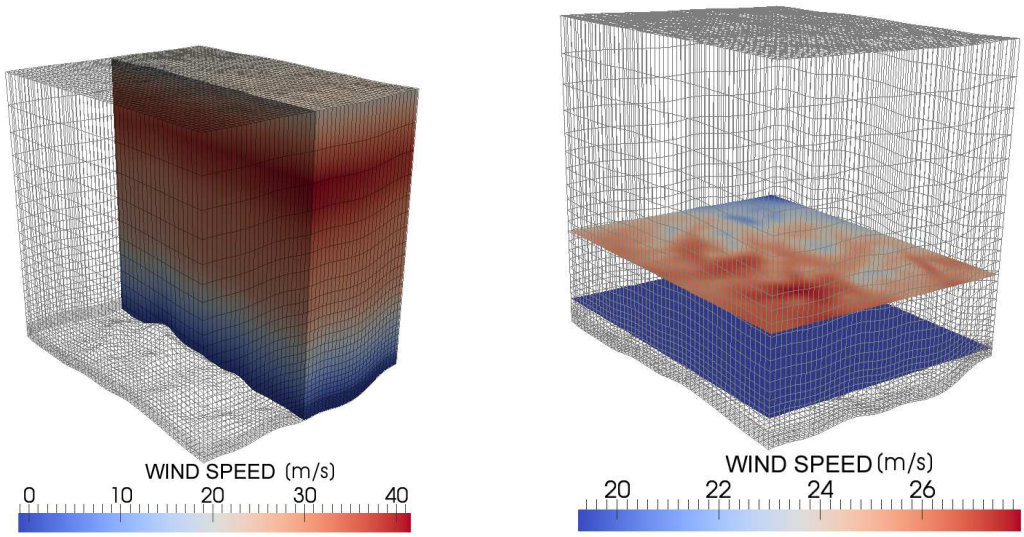


Figure 1.3: Contours of velocity magnitude with respect to altitude around Ankara shown on y (left) and z (right) plane cuts

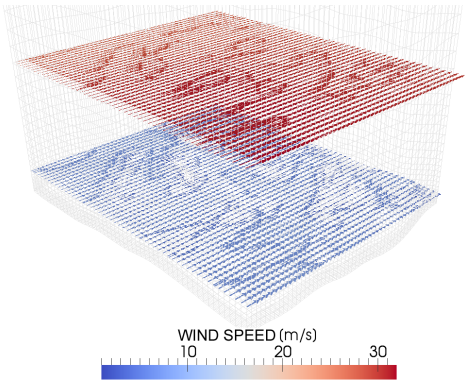


Figure 1.4: Wind speed vectors shown on a z-plane cut

Navier-Stokes solvers are sought out because of their flexibility of using additional equations such as dispersion models and their ability to be used in any flowfield with boundary conditions. In addition a high resolution mesh adequate for the discretization of the flowfield is required.

GAMBIT is a commercial software package designed to help analysts and designers build and mesh models for computational fluid dynamics (CFD) and other scientific applications[21]. It can receive user input by means of GUI (Graphical User Interface) and also by journal files.

FLUENT is a well-known commercial software for modeling fluid flow and heat transfer in complex geometries[22]. It has several tools like UDF(User Defined Function)s with which the user can define unsteady boundary conditions; PROFILE type boundary conditions to specify flow properties varying spatially; and INTERPOLATE option for initializing the flowfield according to discrete point data. These tools are utilized in this study.

The objective of this study is to develop a methodology to carry out unsteady and turbulent atmospheric flow solutions for a given region using MM5 weather prediction data for unsteady spatially varying boundary conditions. Usage of implicitly formulated Navier-Stokes equations has advantage of increasing the resolution without paying attention to Courant number instabilities which will either decrease the time resolution of the simulation or increase the simulation time exponentially. Also, swirls around building models might be simulated using unstructured meshes if the data for buildings are present. The merits of this method will be discussed further in the Results and Discussion chapter.

# CHAPTER 2

# METHODOLOGY

In this study; unsteady weather forecast data of Ankara for a day is obtained in time intervals varying from 1 hour to 5 minutes via MM5. For this process, time dependent boundary and initial conditions from ECMWF (European Centre of Medium Range Weather Forecast) and terrain data from USGS (United States Geographical Survey) are used.

High resolution, structured or unstructured grids are generated via GAMBIT depending on whether high-rise building models are present or not using the topographical data obtained from the MM5 weather forecast data.

Using the weather forecast data, time dependent boundary conditions are utilized and unsteady turbulent Navier-Stokes flow solutions for a day are carried out via FLUENT. A basic flowchart representing the process is given in Figure 2.1.

Detailed information about obtaining MM5 solutions, discretization of the flowfield, boundary conditions and unsteady FLUENT solutions are given in the following sections.

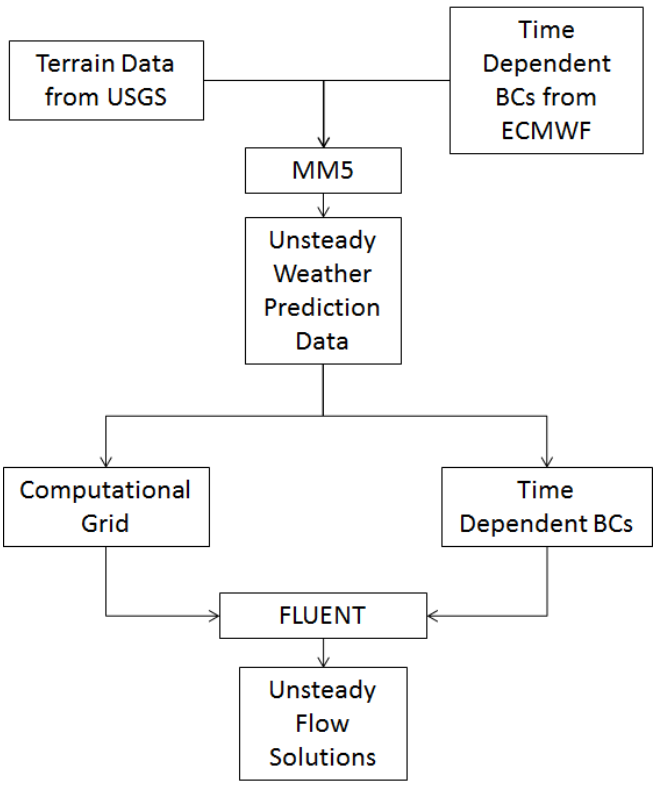


Figure 2.1: Basic flowchart for the computational method

## 2.1 MM5 SOLUTIONS

MM5 solutions can be carried out as follows: time dependent boundary and initial conditions for a zone including the region of interest can be obtained from ECMWF in GRIB file format. TERRAIN, a sub-program of MM5, gets the geographical data from USGS for the region specified for the MM5 run. After that; initial conditions, boundary conditions and terrain data are passed down to PREGRID and REGRIDDER to arrange the initial and boundary conditions for the region of interest. INTERPF changes the vertical altitude to sigma levels as MM5 uses sigma levels for the solution process. For the final step before the solution, NESTDOWN is used to create nests each of which has three times higher horizontal resolution than the previous. A detailed flowchart for obtaining MM5 weather prediction data can be seen in Figure 2.2.

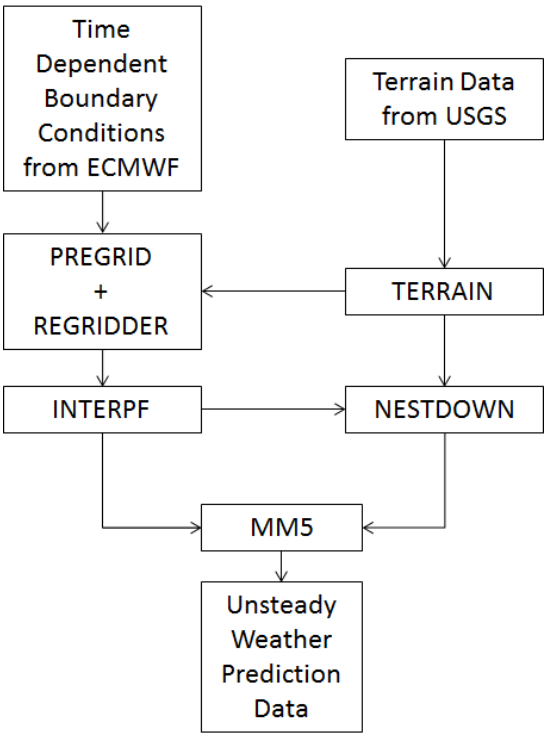


Figure 2.2: Flowchart for MM5 solutions

The limiting factors for the resolution of MM5 weather forecast data are computational resources, CFL (Courant Number) instabilities and resolution of terrain data obtainable from USGS. For consideration; maximum resolution terrain data for Ankara region obtainable from USGS free is 800 meters. Also, decreasing the time step size for the MM5 solution demands increasing the horizontal resolution because of numerical instabilities thus severely increases computational resources. So, the horizontal resolution for MM5 is decided as 800 meters whereas vertical resolution of MM5 is increased as far as 75 meters for the sigma levels in the vicinity of the topography and time step size for the MM5 solution is pushed as low as 5 minutes, just before the CFL instabilities occur for the MM5 solution in Ankara region.

After obtaining time-dependent flow solutions from MM5; data for latitude, longitude, altitude, velocity components are extracted from each node in MM5 domain for each time step. For instance, the location of MM5 nodes for Ankara region are shown in Figure 2.3.

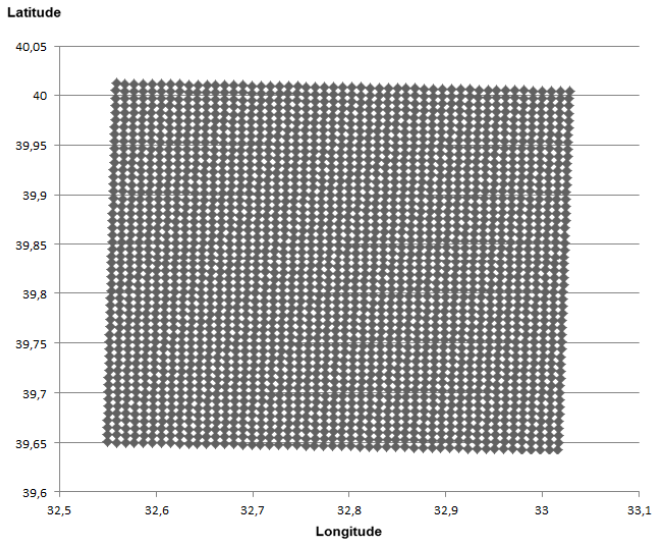


Figure 2.3: Location of MM5 nodes around Ankara region

As the location of the nodes are represented with latitudes and longitudes a transformation to meters is required. Using FransonCoordTrans (v2.3), data obtained from the MM5 solution gives out a cartesian coordinate system of approximately 800 meter horizontal resolution as expected.

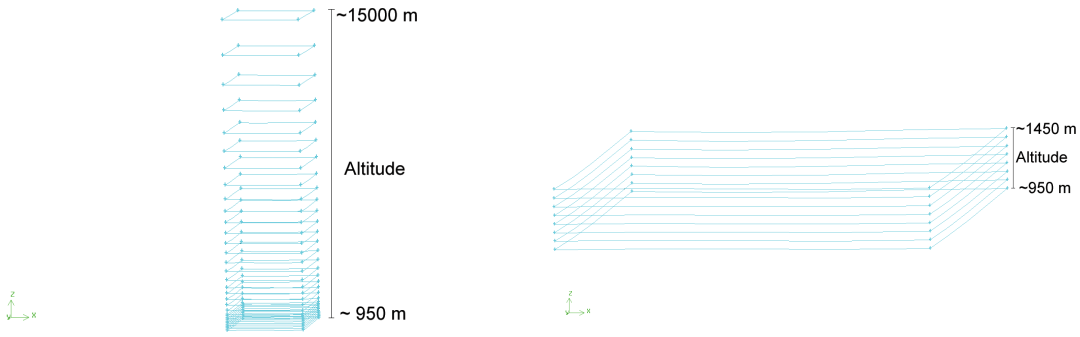


Figure 2.4: All (right) and first 8 (left) sigma levels around METU campus

The first 8 sigma levels which defines the vertical resolution of MM5 weather prediction data has a nearly uniform height (approximately 75m) which are relatively small compared to other sigma levels. For illustration, all sigma levels around METU

campus and the first 8 sigma levels are presented in Figure 2.4.

Accordingly, solving for the region 500 meter above the topography which includes these 8 sigma levels is more beneficial in terms of using most of the MM5 data while not solving for unnecessary regions which increases calculation time.

## 2.2 DISCRETIZATION OF THE SOLUTION DOMAIN

For discretization of the FLUENT solution domain, an interface program in FORTRAN is written which takes latitude-longitude ranges of the solution domain, resolution of the computational grid, unsteady weather prediction data, data for high-rise buildings and size function growth rate (if any high-rise buildings are present) as inputs and creates GAMBIT vertex data file and a GAMBIT journal file which reads the vertex data file to mesh the solution domain. A flowchart representing the process is given in Figure 2.5.

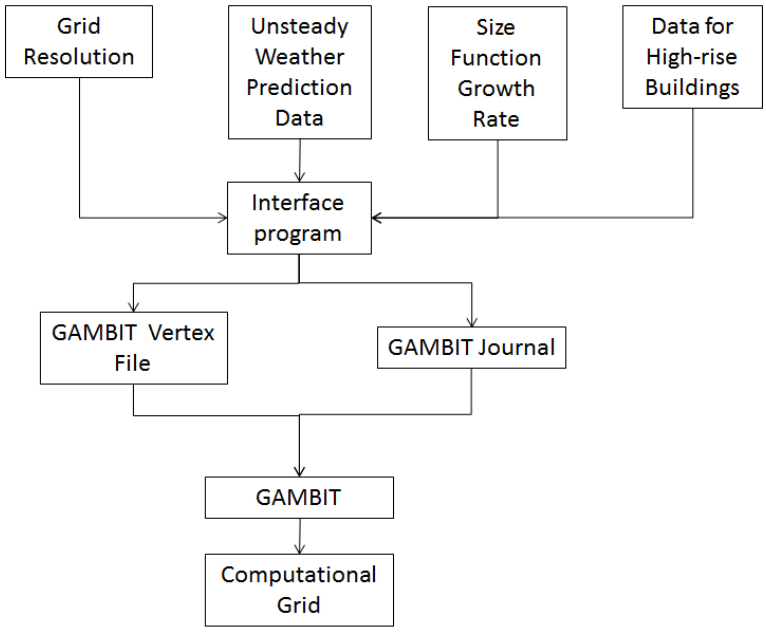


Figure 2.5: Flowchart for discretization of FLUENT solution domain

First, MM5 nodes in the solution domain are determined by the interface program

using the latitude-longitude ranges of the solution domain.

Afterwards, east distance, north distance and altitude (all in meters) of the nodes in the solution domain are written in the form of the GAMBIT vertex import file format by the interface program.

Then via the GAMBIT journal file which is written by the interface program, the vertex data file is read and a model for the topography is generated via GAMBIT's Import Vertex Data and Create Surface from Vertex Rows options using information for the nodes at ground level. Using the same procedure described for the ground surface; the surface for the 8th sigma level is generated bounding the solution domain from above.

The approach for meshing the solution domain differs if there are building models present in the solution domain. Structured mesh is preferred over unstructured as the number of cells for meshing the flowfield is significantly less for a given vertical resolution. But if the geometry to be modeled is complex such as if there are any building models present, usage of unstructured mesh is more beneficial. Below subsections describe the approaches for meshing the flowfield for both cases.

### 2.2.1 DISCRETIZATION OF SOLUTION DOMAIN OVER TOPOGRAPHICAL TERRAIN

Meshing of the solution domain when there are no building models present is straight forward compared to the case with building models. As the geometry to be modeled is not complex, structured mesh can be used.

First thing the GAMBIT journal file does is to mesh the upper and lower boundaries of the flowfield using an appropriate resolution given as input to the interface program. Then, side edges of the flowfield are meshed with an appropriate resolution given as

input to the interface program.

Using this approach, the vertical resolution can be increased as much as desired, independently of the horizontal resolution and without increasing the number of cells exponentially as structured mesh is used for the flowfield with only topography. Other important factors when deciding the vertical resolution is that the nodes of MM5 in the FLUENT solution domain should coincide with the vertexes of cells created by GAMBIT to minimize the interpolation errors and because of the surface roughness model that will be used in this study, the maximum vertical resolution in the ground level should be higher than 1 meter as will be explained later.

### 2.2.2 DISCRETIZATION OF SOLUTION DOMAIN OVER TOPOGRAPHICAL TERRAINS WITH HIGH-RISE BUILDING MODELS

The approach for meshing the solution domain is different when there are buildings present in the region to be solved as the model of topography should be modified because of the buildings. For that; the locations, orientation and the sizes of the buildings should be known.

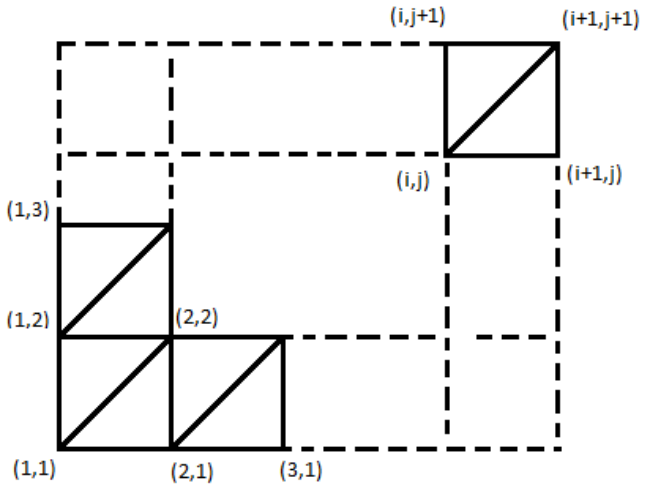


Figure 2.6: Edges of the triangular surfaces for approximating the topography

The interface program mentioned previously, which takes these data as inputs, is written for generating the topography with buildings. Even if these data are provided, the altitudes which the building models intersect with the buildings is difficult to find.

Using the fact that 3 points in space represents a plane, the surface is divided into triangle surfaces using (i,j) , (i+1,j), (i+1,j+1) nodes for the lower triangle and (i,j), (i+1,j+1), (i,j+1) nodes for upper triangle as seen in Figure 2.6 approximating topography.

After that, the code finds in which region each of the buildings' lower edges resides. And using equation of a plane passing through 3 points the altitudes which the building models intersect with the topography are found.

After that, the building models are shifted vertically by the lowest altitude of the edges of the building for coinciding all the lower edges with the topography. Subtracting the building models from the previously generated solution domain for the case without building models, a solution domain with building models is generated.

Meshing these kind of geometries can be tricky as the resolution around the building models should be more to capture swirls caused by buildings and that high resolution grids increases the number of cells immensely. Also, the geometry to be meshed is complex. So, GAMBIT size functions and unstructured grids are used to overcome these problems.

GAMBIT's size functions allow the user to control the size of the mesh in regions surrounding a specified entity. Specifically, they can be used to limit the mesh-interval size on any edge or the mesh-element size on any face or volume. Growth rate defines the increase in mesh-element edge length with each succeeding layer of elements. Source defines the starting entity of the reduction or enlargement of the mesh sizes whereas Attachment defines the ending entity. Size limit restricts the maximum or

minimum lengths of edges of the meshes.

For discretizing the solution domain with high-rise buildings, the following approach is used. Firstly, faces of the building models are meshed with a high resolution (for example 5 meters). After that, an enlarging (growth rate $> 1$) size function with a maximum edge length equal to the horizontal resolution from the lower edges of the building models (source) to the topography surface (attachment) is created to mesh the surface with building models.

Having meshed the topography; another enlarging size function is generated with a maximum edge length equal to the vertical resolution from the surface with building models to the 8th sigma level which is the upper bound for the flowfield.

## 2.3 INITIAL AND BOUNDARY CONDITIONS

Implementing the MM5 weather forecast data as boundary conditions is complicated as FLUENT does not have a tool for implementing boundary conditions varying with both time and space and the data is only obtainable at the MM5 nodes in the region of interest thus discrete and also varies with time.

FLUENT has an interpolation tool which initializes the flowfield according to interpolation of point data provided and a boundary profile tool which can read and write the flow properties in a defined boundary. Also the profiles can be hooked to boundaries. Whereas these tools are adequate for a steady simulation, it may not be the case for the unsteady case. Consider that a simulation will be done for one day and the weather forecast data for that day is given for 5 minute intervals which is the maximum time resolution for the weather forecast for Ankara as explained in the MM5 solutions section. 1+(60/5)*24 = 289 point data interpolation files will be needed to get 289 sets of boundary condition profiles which will be really tiresome work as the intervals at which the weather forecast data is obtained gets smaller.

To handle these difficulties; the interface program reads the weather forecast data, writes the FLUENT interpolation files for each of time intervals MM5 solutions are obtained, then creates a FLUENT journal file to read them to initialize the solution domain and finally writes boundary profiles named according to the time interval they are created for.

A flowchart for acquiring time dependent boundary condition profiles is given in Figure 2.7.

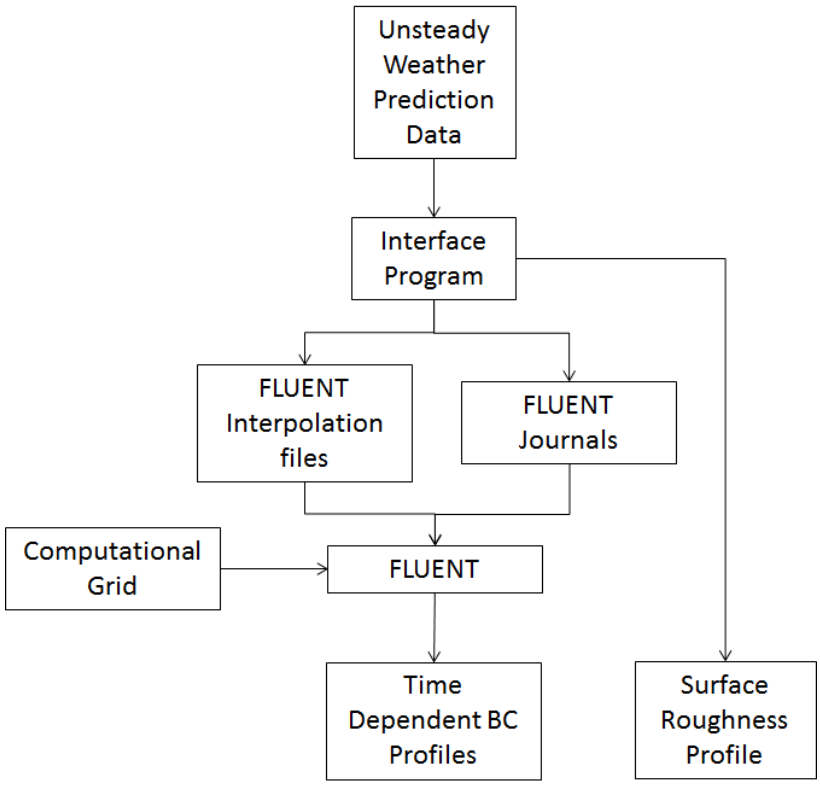


Figure 2.7: Flowchart for obtaining time dependent boundary condition profiles

It is decided to use spatially and time varying velocity inlets for the boundary conditions of the side and upper surfaces to utilize most of the data available from MM5.

For the topography, a no-slip no heat flux wall is used. For the topographical terrain with no building models, roughness model can be obtained from MM5 and is included in the solution with no building models.

For the flowfield with building models, a simple no heat flux wall without roughness model is taken as boundary condition.

### 2.3.1 INTERPOLATION OF MM5 SOLUTION AND OBTAINING VELOCITY PROFILES AT BOUNDARIES

Flow properties (three dimensional velocity components, pressure) at boundaries and inside of the solution domain are written in FLUENT's INTERPOLATE file format to initialize the domain according to the MM5 solution and to determine the boundary conditions for each time interval.

After the initialization part, determination of the spatially varying unsteady boundary conditions is done by using FLUENT to write the profiles at the velocity inlets for each time interval. Interpolation and writing the profiles for each solution of MM5 at all time intervals is done automatically by using a FLUENT journal file which is created by the interface program according to the inputs. For identifying which BC profile belongs to which time interval, each BC profile is named accordingly as they will be read by the UDFs (User Defined Functions) explained in the Unsteady FLUENT solutions section.

### 2.3.2 SURFACE ROUGHNESS MODEL

Terrain features such as vegetation, buildings, lakes are modeled as surface roughness in numerical simulations. FLUENT can use surface roughness constant and surface roughness length at wall boundaries to account for the unevenness of the wall. Surface roughness constant is 0.5 by default which is for smooth surfaces. But as the

topography is rough, it can be taken between 0,5 and 1. USGS terrain data also includes terrain type information which can be used, if the LANDUSE option in MM5 is activated. A table showing these categories and corresponding roughness lengths and terrain types can be seen in Table 2.1.

| Category | Roughness Length(cm) | Terrain Type |
|---|---|---|
| 1 | 50 | Urban and Built-Up Land |
| 2 | 15 | Dryland Cropland and Pasture |
| 3 | 15 | Irrigated Cropland and Pasture |
| 4 | 15 | Mixed Dryland/Irrigated Cropland and Pasture |
| 5 | 14 | Cropland/Grassland Mosaic |
| 6 | 20 | Cropland/Woodland Mosaic |
| 7 | 12 | Grassland |
| 8 | 10 | Shrubland |
| 9 | 11 | Mixed Shrubland/Grassland |
| 10 | 15 | Savanna |
| 11 | 50 | Deciduous Broadleaf Forest |
| 12 | 50 | Deciduous Needleleaf Forest |
| 13 | 50 | Evergreen Broadleaf Forest |
| 14 | 50 | Evergreen Needleleaf Forest |
| 15 | 50 | Mixed Forest |
| 16 | 0.01 | Water Bodies |
| 17 | 20 | Herbaceous Wetland |
| 18 | 40 | Wooded Wetland |
| 19 | 10 | Barren or Sparsely Vegetated |
| 20 | 10 | Herbaceous Tundra |
| 21 | 30 | Wooded Tundra |
| 22 | 15 | Mixed Tundra |
| 23 | 10 | Bare Ground Tundra |
| 24 | 5 | Snow or Ice |

Table 2.1: USGS LANDUSE Categories

Using this information, surface roughness lengths at the node points of MM5 in the solution domain can be extracted and via the interface program, surface roughness profile for topography of the solution domain can be obtained. But an important aspect for determining the vertical resolution is that the minimum vertical dimension for the cells on the topography should exceed twice the roughness length according to FLUENT user manual. So, the maximum vertical resolution should be 1 meter.

## 2.4 UNSTEADY FLUENT SOLUTIONS

Unsteady FLUENT solutions can be carried out using the computational grid, unsteady boundary conditions profiles and surface roughness profile (if available) with the help of UDFs.

Firstly, computational grid with the specified boundary conditions is passed down to FLUENT. After that, surface roughness profile is defined and hooked to the topography which is defined as a wall. Then, an appropriate time step size and iteration per time step is selected and solution settings are utilized. When iterating in time, UDFs gets the simulation time and reads the BC profiles in adjacent times just before and after. Then UDFs linearly interpolates the values for each cell for that time step using information obtained from these profiles. Flowchart for unsteady FLUENT solutions can be seen in Figure 2.8.

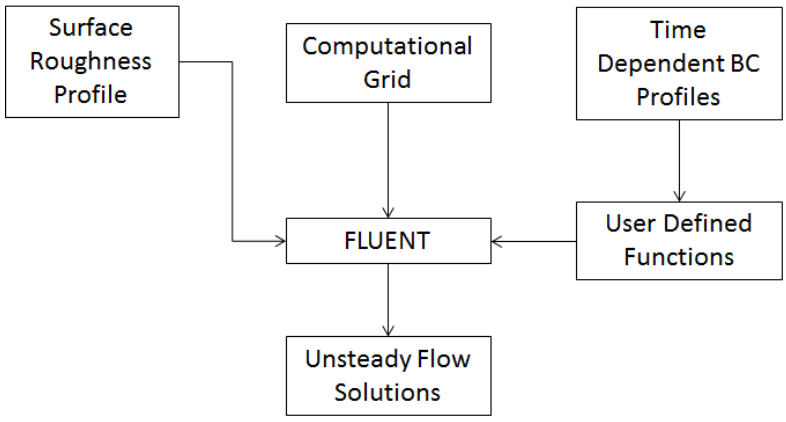


Figure 2.8: Flowchart for unsteady FLUENT Solutions

### 2.4.1 USER DEFINED FUNCTIONS (UDFS) FOR TIME AND SPATIALLY VARYING BOUNDARY CONDITIONS

After the time dependent boundary condition profiles are created, they can be hooked to the boundaries at appropriate time steps by the user but this approach limits the time step size that will be used in the simulation which can cause divergence issues

and also is really tiresome if the weather forecast data is obtained for small time intervals (for example 5 minutes) as mentioned earlier.

For that, four User Defined Functions (UDFs) for three velocity components at the velocity inlets are written to interpolate the boundary conditions linearly in time according to the unsteady BC profiles.

Firstly these UDFs loop around the faces of cells on the boundary they were attached to get the number of faces on that boundary using F-LOOP macro. Next, the UDFs gets the solution time using CURRENTTIME macro. Using the simulation time, the code determines the previously generated unsteady BC profiles written for adjacent times and reads them. After that, they interpolate the all the values on the faces linearly in time. Finally, it identifies the locations of the faces and imposes the interpolated values using F-PROFILE function.

For example if the simulation time is 450 seconds and unsteady BC profiles are created at 5 minute intervals, UDFs identify and reads the profiles for t = 300 seconds and t = 600 seconds storing the information at the all the faces of the boundary they are attached to then interpolates the values at each of the cells linearly in time. After that, it identifies the locations of faces and imposes the interpolated values for each face on that boundary at t=450 seconds.

### 2.4.2 SOLVER SETTINGS AND ASSUMPTIONS

3 dimensional Reynolds Averaged Navier-Stokes equations which are basically conservation of mass and momentum are solved using FLUENT. K-E RNG model with standard wall functions is used to account for the turbulence as in literature it is known to give good results for atmospheric flow modeling.

RANS equations are as follows:

$$\frac{\partial \rho}{\partial t} + \frac{\partial}{\partial x_i}(\rho u_i) = 0 \tag{2.1}$$

$$\frac{\partial}{\partial t}(\rho u_i) + \frac{\partial}{\partial x_j}(\rho u_i u_j) = -\frac{\partial p}{\partial x_i} + \frac{\partial}{\partial x_j}\left[\mu\left(\frac{\partial u_i}{\partial x_j} + \frac{\partial u_j}{\partial x_i} - \frac{2}{3}\delta_{ij}\frac{\partial u_l}{\partial x_l}\right)\right] + \frac{\partial}{\partial x_j}(-\rho\overline{u_i' u_j'}) \tag{2.2}$$

As the velocities are small, air is assumed to be incompressible and above equations reduce to;

$$\frac{\partial}{\partial x_j}(\rho u_j) = 0 \tag{2.3}$$

$$\frac{\partial u_i}{\partial t} + u_j\frac{\partial u_i}{\partial x_j} = -\frac{1}{\rho}\frac{\partial p}{\partial x_i} + \nu\frac{\partial^2 u_i}{\partial x_j \partial x_j} - \frac{\partial \overline{u_i' u_j'}}{\partial x_j}. \tag{2.4}$$

Reynold Stresses are calculated as (according to bousinesq approach):

$$-\rho\overline{u_i' u_j'} = \mu_t\left(\frac{\partial u_i}{\partial x_j} + \frac{\partial u_j}{\partial x_i}\right) \tag{2.5}$$

Where $\mu_t$ is:

$$\mu_t = \rho C_\mu \frac{k^2}{\epsilon} \tag{2.6}$$

k and $\epsilon$ are calculated as:

$$\frac{\partial}{\partial t}(\rho k) + \frac{\partial}{\partial x_i}(\rho k u_i) = \frac{\partial}{\partial x_j}\left(\alpha_k \mu_{\text{eff}}\frac{\partial k}{\partial x_j}\right) + G_k - \rho\epsilon \tag{2.7}$$

$$\frac{\partial}{\partial t}(\rho\epsilon) + \frac{\partial}{\partial x_i}(\rho\epsilon u_i) = \frac{\partial}{\partial x_j}\left(\alpha_\epsilon \mu_{\text{eff}} \frac{\partial k}{\partial x_j}\right) + C_{1\epsilon}\frac{\epsilon}{k}(G_k) - C_{2\epsilon}\rho\frac{\epsilon^2}{k} \tag{2.8}$$

where $G_k$ represents the generation of turbulence kinetic energy due to the mean velocity gradients and calculated as:

$$G_k = -\rho\overline{u_i' u_j'}\frac{\partial u_j}{\partial x_i} \tag{2.9}$$

and model constants are:

$$C_{1\epsilon} = 1.42, \quad C_{2\epsilon} = 1.68 \tag{2.10}$$

The atmospheric flow is assumed to be incompressible as density variations between ground and approximately 500 meters above are negligible.

Second order discretization methods for momentum and continuity equations are utilized to minimize the numerical errors as the simulation will be run for 24 hours. Node based discretization methods are used to increase the accuracy without increasing the number of cells which effects the solution time.

Implicit solver is used to preserve the robustness of the solution while changing time step sizes. Pressure velocity coupling is handled by SIMPLE algorithm[23]. Pressure based solver is used as the velocities in the flowfield are small in magnitude.

Gravity and buoyancy effects are neglected as they cause instabilities for the solution.

# CHAPTER 3

# RESULTS AND DISCUSSION

In this study; unsteady and turbulent atmospheric flow solutions are carried out for the solution domain over topographical terrain and over topographical terrain with high-rise building models as described in the Methodology section.

For the solution domain over topographical terrain; structured grids with 25 meter horizontal and 15 meter vertical resolution is generated. After utilizing time dependent boundary conditions, hourly atmospheric flow solutions are presented for a day. Afterwards, comparison of hourly solutions with MM5 is done. In addition, velocity profiles in the middle of the domain for FLUENT solutions are compared with MM5 solutions. Finally, effects of surface roughness model are investigated.

For the solution domain over topographical terrain with high-rise building models; unstructured grids with vertical and horizontal resolution varying from 5 meter (around building models) to 80 meter (further away from the models) is generated. Hourly atmospheric flow solutions with high-rise building models are presented for a day.

The simulation is done for the date of 15th of June in 2010 starting from 18:00 till 16th of June 18:00. For that day, sunset and sunrise moments of METU campus are acquired from www.sunrisesunsetmap.com as 05:20 and 20:19 respectively.

MM5 weather forecast data for that day occupy 1 GB of memory when the data is

obtained for 5 minute time intervals. Also the FLUENT interpolation files for 5 minutes interval data from MM5 holds up 22KB * 289 = 6358 KB of memory. Time dependent boundary condition profiles hold up 726 MBs for 5 minute intervals case.

One of the limitations on the solution time is the unavailability of parallel computing at the moment. FLUENT has also a tool for parallelizing the computations but when doing so it splits the solution domain to parts equal to the number of processors. Because of this, the cells in the boundaries of the flowfield are re-identified. So, usage of the previously mentioned UDFs results in rewriting the flow properties at the cells on the boundary again and again, thus producing wrong boundary conditions.

25 meter horizontal and a 15 meter vertical resolution flowfield simulations with only topography are obtained in approximately 10,5 hours in a Corei7 3.40 Ghz computer with 4 GB RAM. Flowfield simulations with building models and resolution varying from 5 meters around the buildings to 80 meters are obtained in approximately 14.5 hours as the convergence is smaller due to the disturbances in the flowfield because of the building models and high resolution around them.

## 3.1 UNSTEADY ATMOSPHERIC FLOW SOLUTİONS OVER TOPOGRAPHICAL TERRAIN

For case study; METU campus area is selected. Latitude and longitude ranges of the METU campus are obtained as 39.66 N - 40.00 N and 32.55 E - 33.00 E from Google Earth. Using the interface program as mentioned in the Methodology section, nodes in the MM5 solution domain (Ankara) containing the region of METU campus are determined as seen in Figure 3.1. For a better illustration, close-up view of the FLUENT solution domain and METU campus are given in Figure 3.2 along with the MM5 nodes on the topography in the FLUENT solution domain (METU Campus).

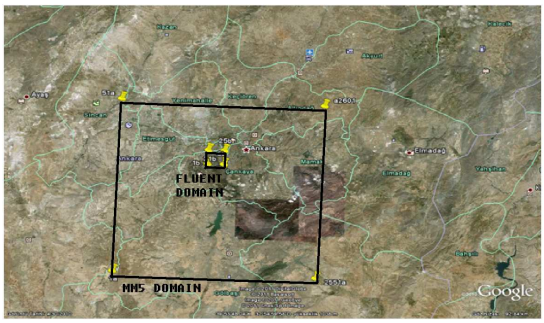


Figure 3.1: Borders of MM5 and FLUENT solution domains

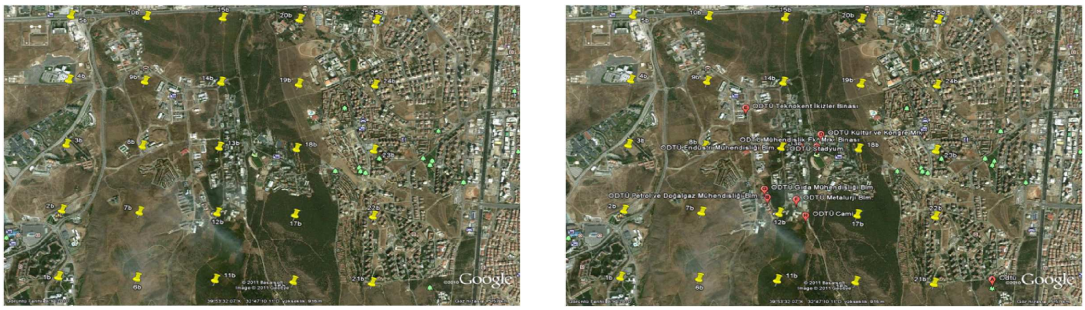


Figure 3.2: Close-up view of FLUENT solution domain (left) and METU campus with MM5 nodes on the topography (right)

Afterwards latitude and longitude data for the MM5 nodes around METU campus are transformed to east and north distances in meters. The upper bound for the FLUENT solution domain is determined as the 8th sigma level to use most of the data MM5 provides without solving for unnecessary regions which increases the solution time as seen in Figure 3.3.

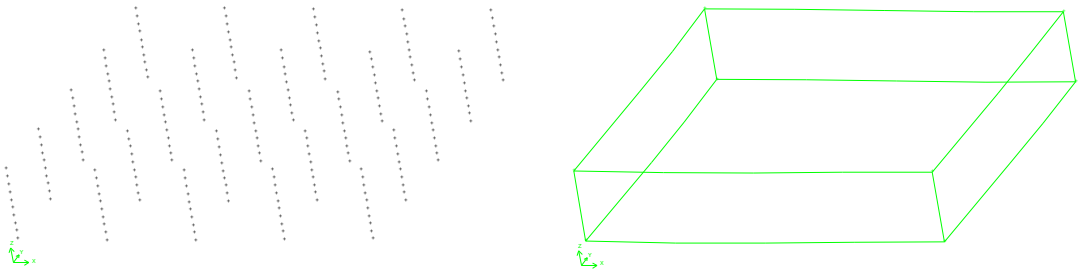

Figure 3.3: MM5 nodes on the first eight sigma levels around METU campus (left) and FLUENT solution domain (right)

Then, GAMBIT vertex data file for these nodes is written and nodes at the ground level are used to create a model for the topography as seen in Figure 3.4.

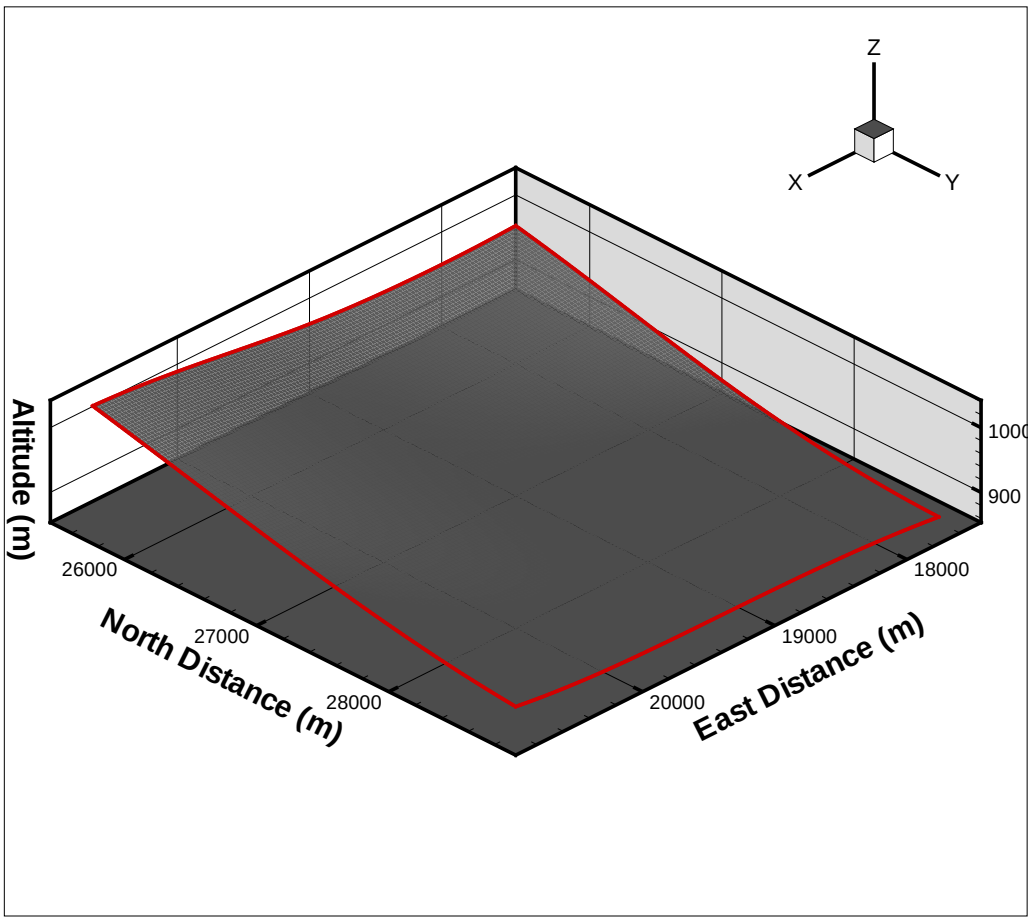


Figure 3.4: Topography model for METU campus

For METU campus case without building models, horizontal resolution is decided as 25 meters as it is a commonly used for wind power applications and vertical resolution is decided as 15 meters which is 5 times more than the resolution for the lowest sigma level height from MM5. For imposing these resolutions; topography and 8th sigma levels are meshed with 25 meter edge lengths whereas side edges are meshed with 15 meter edge lengths as seen in Figure 3.5.

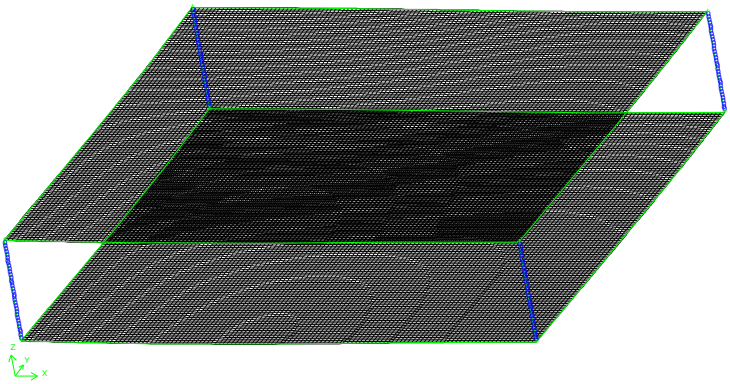

Figure 3.5: Surface meshes and meshed side edges for the FLUENT Solution Domain

After all these steps are done, the domain is discretized with 128x128x35=573440 cells as seen in Figure 3.6.

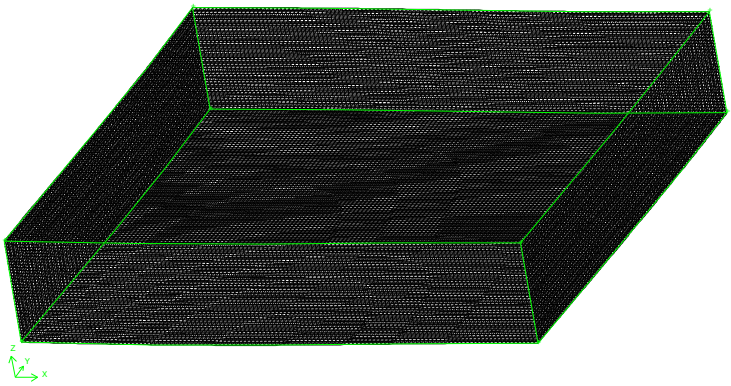

Figure 3.6: Structured grid of the FLUENT solution domain

Flow properties (three dimensional velocity components and pressure) at boundaries and inside of the flowfield around METU campus are written in FLUENT's INTERPOLATE file format to initialize the flowfield according to the MM5 solution and to determine the boundary conditions for each time interval. For example, interpolated values of MM5 nodes in the FLUENT solution domain for the zeroth hour of the simulation which will be also used as initial condition can be seen in Figure 3.7.

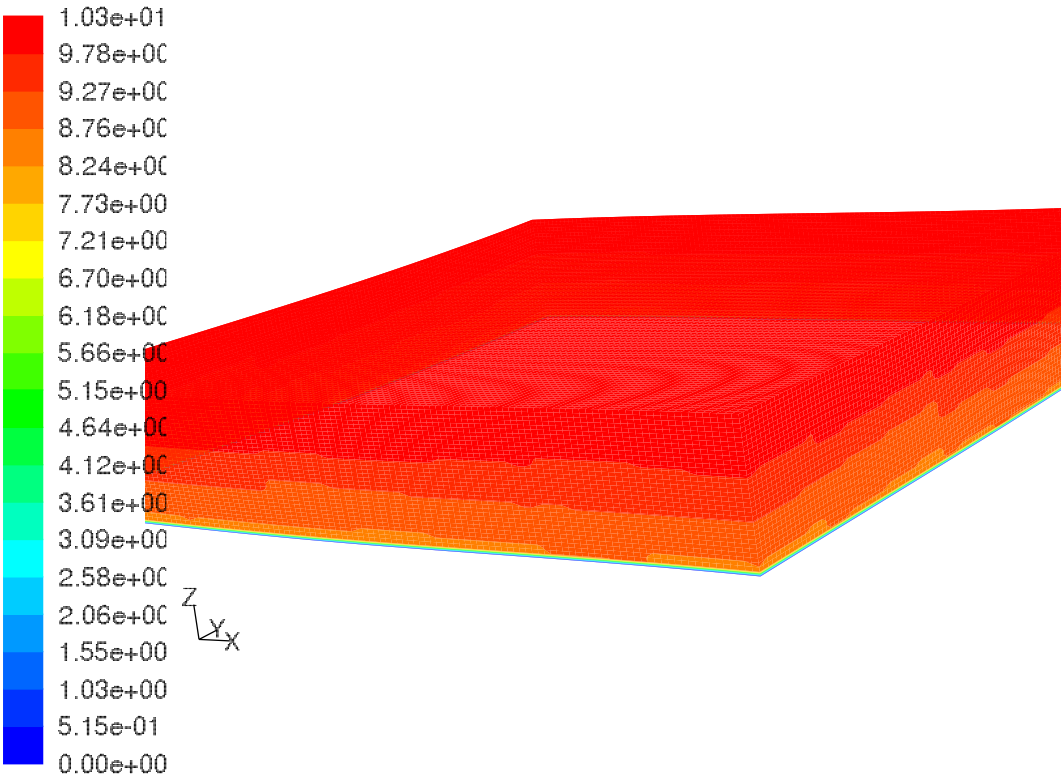


Figure 3.7: Velocity magnitude contours of the FLUENT solution domain at the 0th hour of the simulation

After the initialization part, determination of the spatially varying unsteady boundary conditions is done by using FLUENT to write the profiles at the velocity inlets for each time interval named according to the time they belong to. As an example velocity profiles (colored according to velocity magnitudes) at the 6th and 12th hour of the simulation can be seen in Figure 3.8 and Figure 3.9. Surface roughness constant for the topography is chosen as 0.7 as it is 0.5 for smooth and 1 for very rough surfaces. Furthermore, surface roughness height point profiles obtained from the MM5 solutions via the interface program are used for the topography.

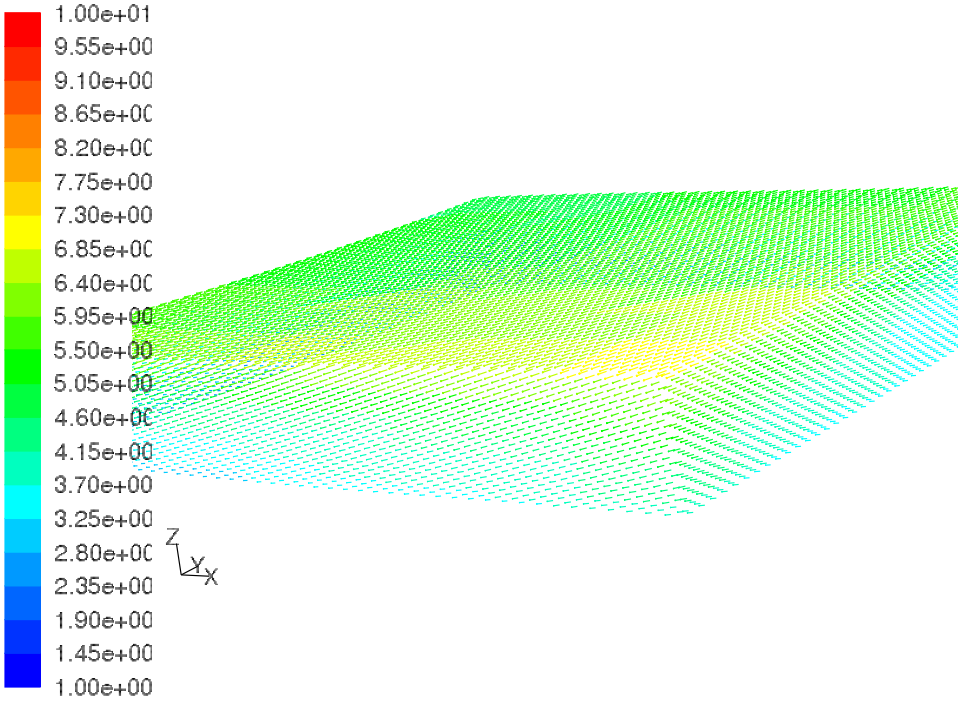


Figure 3.8: Velocity profiles for the velocity inlets at the 6th hour of the simulation

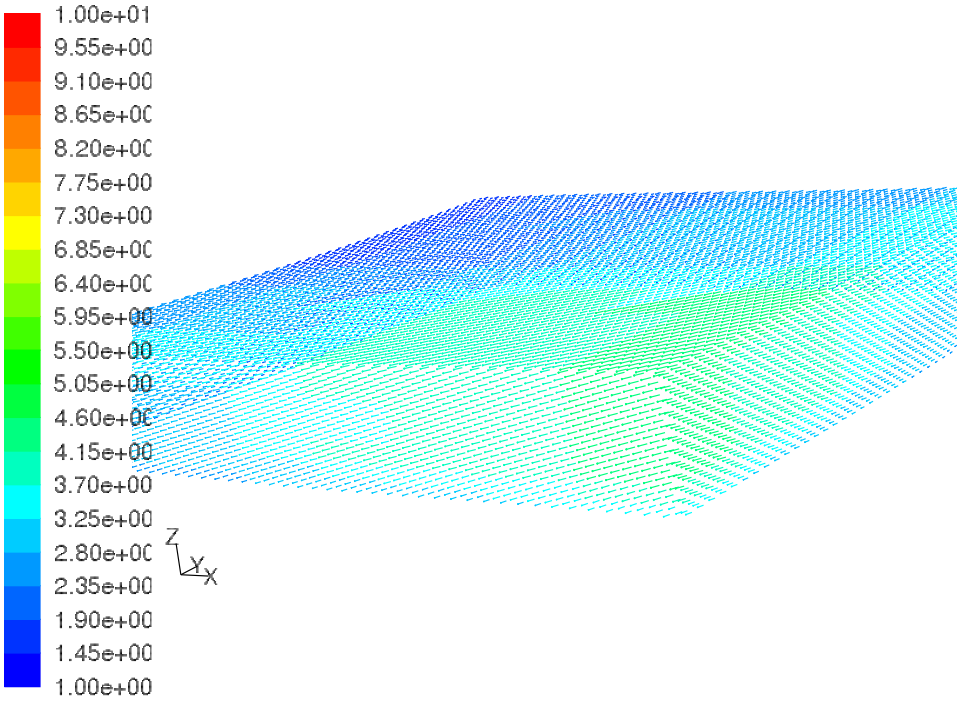


Figure 3.9: Velocity profiles for the velocity inlets at the 12th hour of the simulation

Using the time dependent BC profiles generated and UDFs; unsteady atmospheric flow solutions over METU campus are carried out. Time step size for the simulation is determined as 150 seconds which is half of the time intervals at which MM5 solutions are obtained.

Three terrain following surfaces which are 25,50 and 100 meters above the ground are created to visualize the unsteady solutions. These surfaces are generated using FLUENT's Surface Transform tool to make an exact copy of the topography at specified distances above it. For a more clear illustration, the surfaces are plotted with the FLUENT solution domain as seen in Figure 3.10. Blue, yellow, red are used for the surfaces 25, 50, 100 meter above the ground respectively.

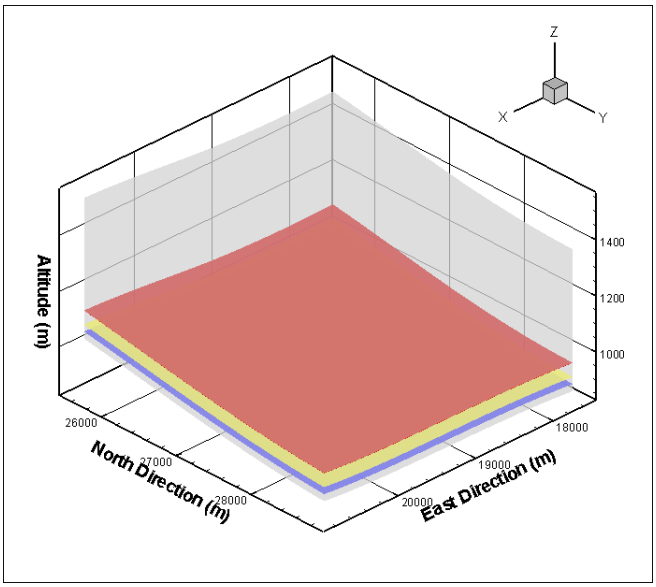


Figure 3.10: FLUENT solution domain with three terrain following surfaces 25, 50 and 100 meter above the ground

### 3.1.1 SIMULATION RESULTS FOR A DAY

Velocity magnitude contours with streamlines at 25, 50 and 100 meters above the ground are presented in Figure 3.11 between 19:00 and 24:00 on 15.6.2010; in Figure 3.12 between 01:00 and 06:00 on 16.6.2010; in Figure 3.13, between 07:00 and 12:00 on 16.6.2010; in Figure 3.14 between 13:00 and 18:00 on 16.6.2010 respectively.

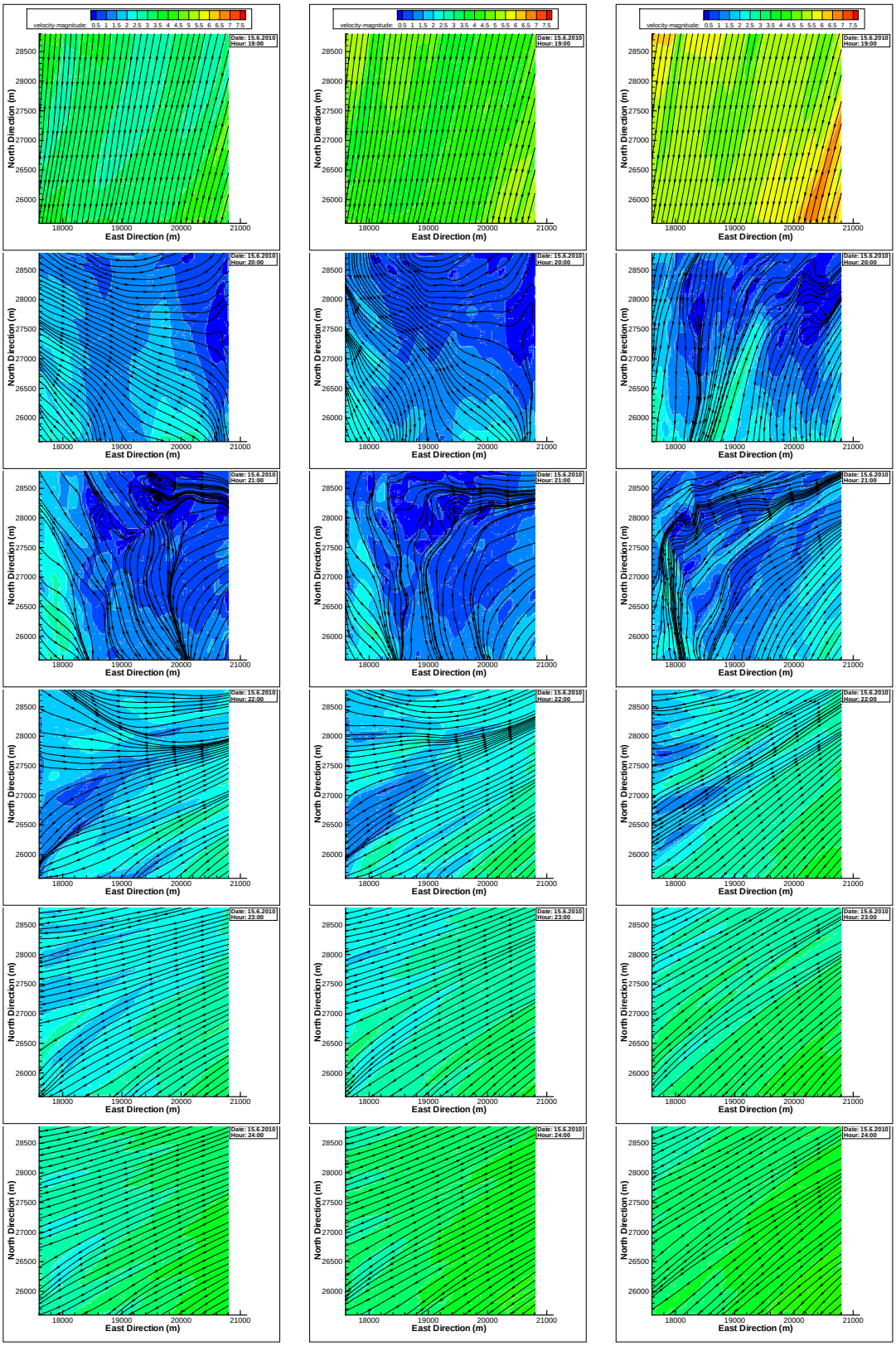


25m above ground 50m above ground 100m above ground

Figure 3.11: Velocity magnitude contours with streamlines 25, 50 and 100m above the ground between 19:00 and 24:00 on 15.6.2010

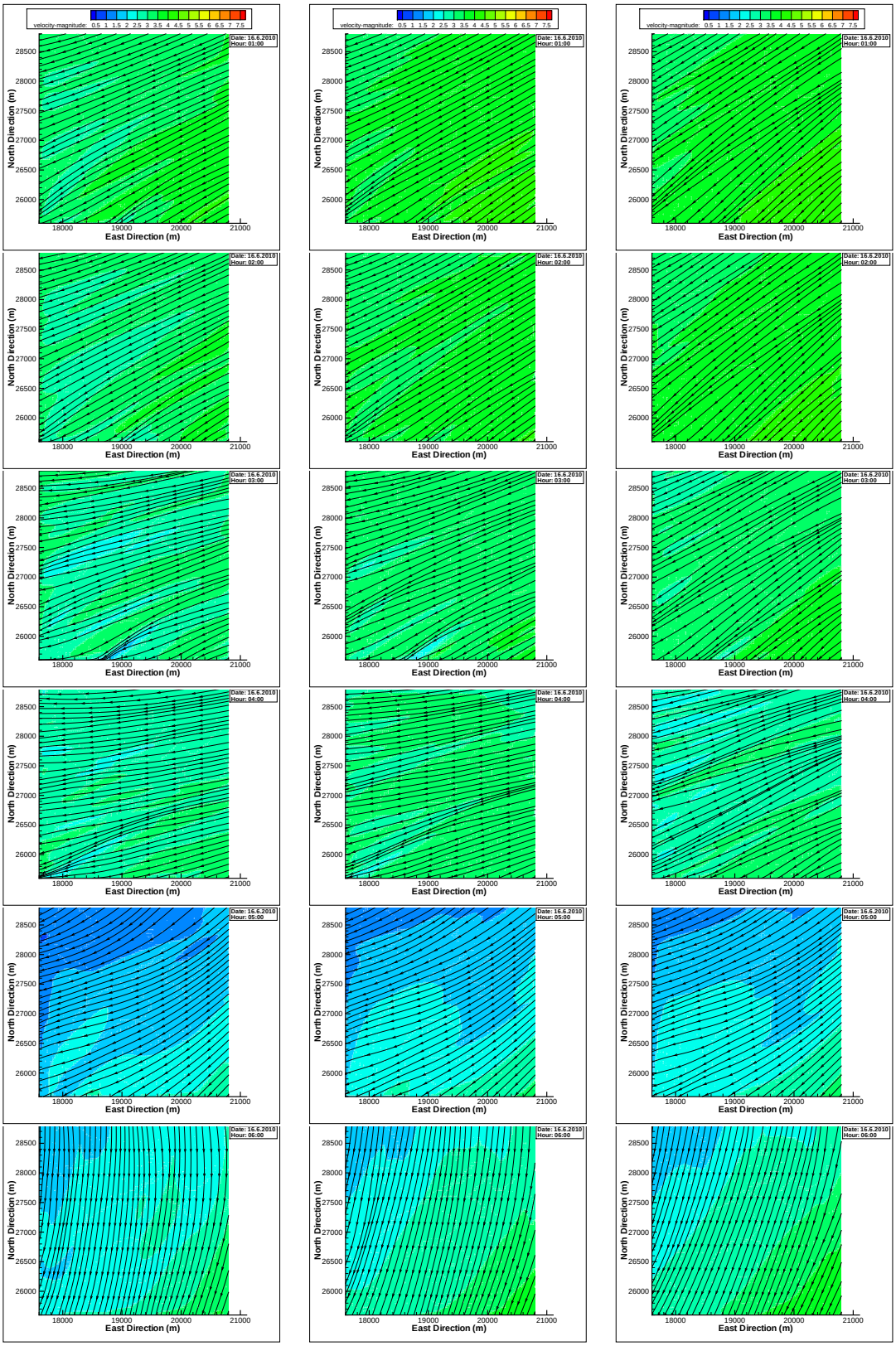


Figure 3.12: Velocity magnitude contours with streamlines 25, 50 and 100m above the ground between 01:00 and 06:00 on 16.6.2010

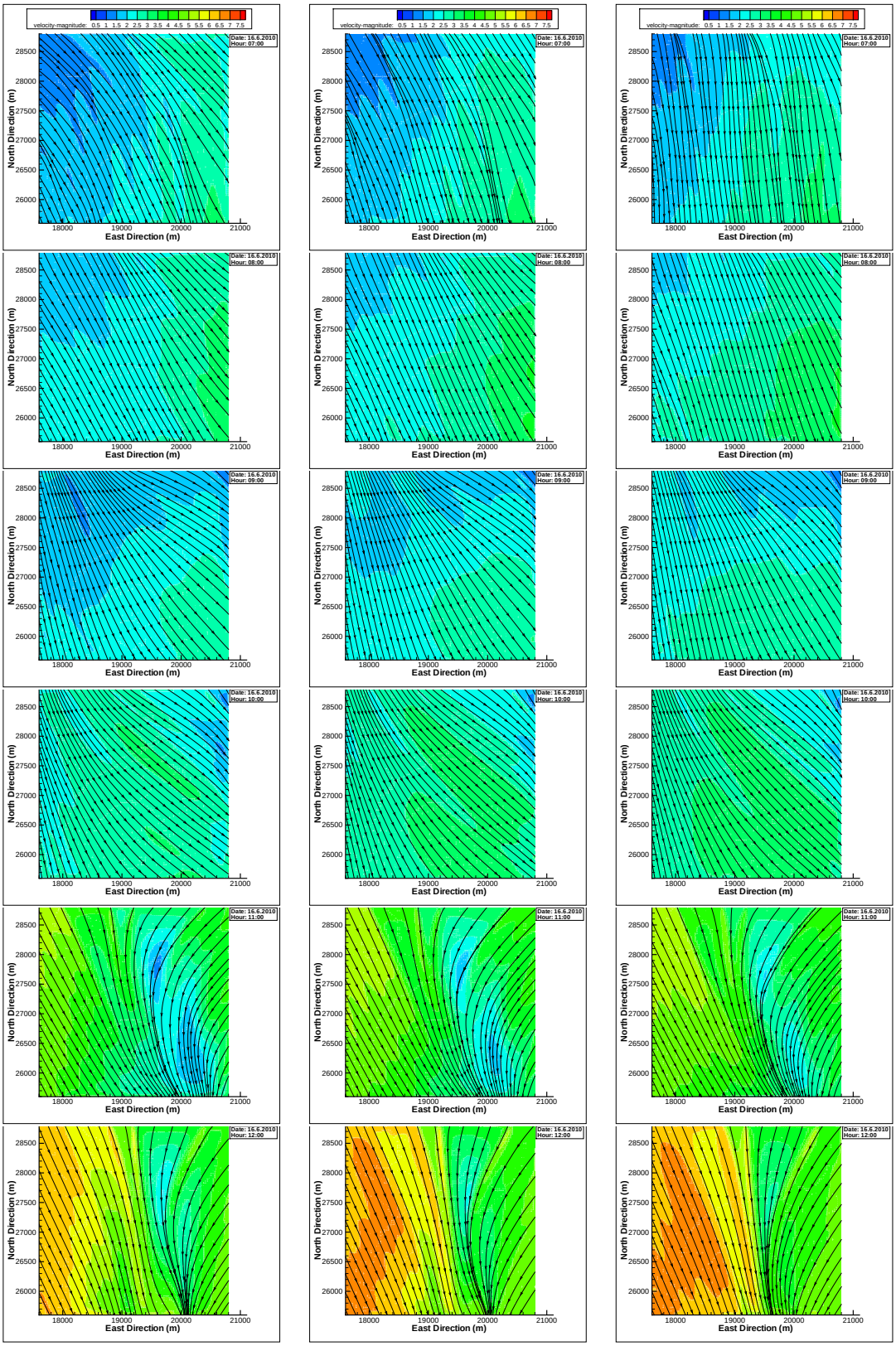


Figure 3.13: Velocity magnitude contours with streamlines 25, 50 and 100m above the ground between 07:00 and 12:00 on 16.6.2010

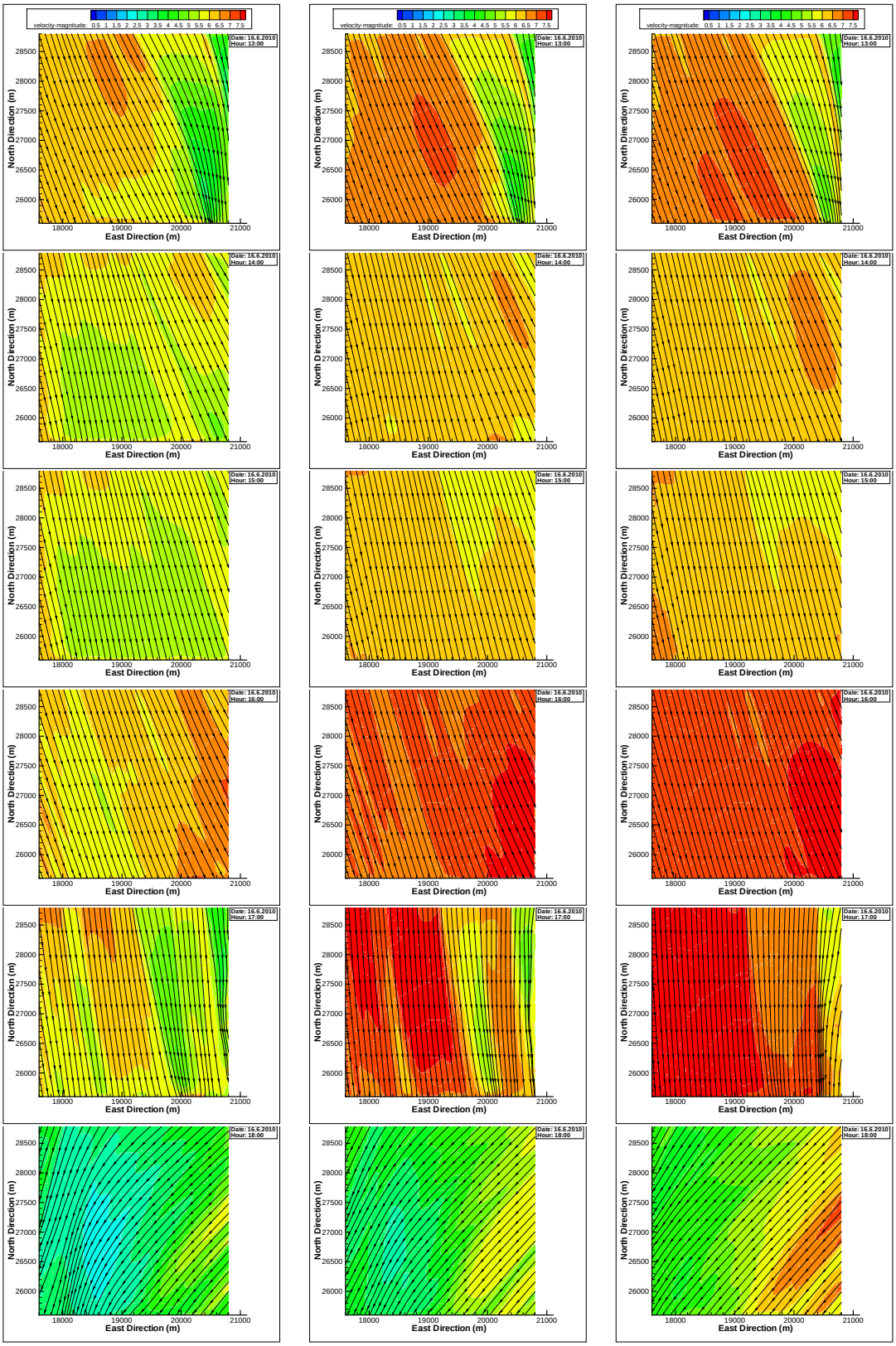


25m above ground 50m above ground 100m above ground

Figure 3.14: Velocity magnitude contours with streamlines 25, 50 and 100m above the ground between 13:00 and 18:00 on 16.6.2010

As seen in Figure 3.11, Figure 3.12, Figure 3.13 and Figure 3.14; wind direction changes with height above the ground and time even when observed at an hourly basis. So; based on MM5 solution, it can be said that assuming a steady wind profile blowing in a single direction may be unrealistic. Also, it is seen that as the height above the ground increases velocity magnitude increases and irregularities in flowfield tend to decrease. It is another observation that velocity magnitudes are higher on elevated grounds even when observed at the same heights above ground.

According to this simulation, abrupt changes in wind direction and speed are observed between 20:00 and 21:00 o'clock on 11.06.2010 and between 6:00 and 7:00 o'clock on 12.06.2010. These changes are thought to occur because of the sunset and sunrise as they are at the same intervals as said previously.

### 3.1.2 COMPARISON OF MM5 SOLUTIONS WITH FLUENT

Solutions of MM5 is compared with FLUENT solutions at the 1st, 3rd, 6th, 12th and 24th hours of the simulation using the same terrain following surfaces 25, 50 and 100 meter above the ground to understand the advantages of this method over MM5 because of the increased resolution. Velocity magnitude contours of FLUENT and MM5 solutions with streamlines at the 1st, 6th, 12th and 24th hours of the simulation at 25, 50 and 100 meters above the ground are presented in Figure 3.15, Figure 3.16 and Figure 3.17 respectively.

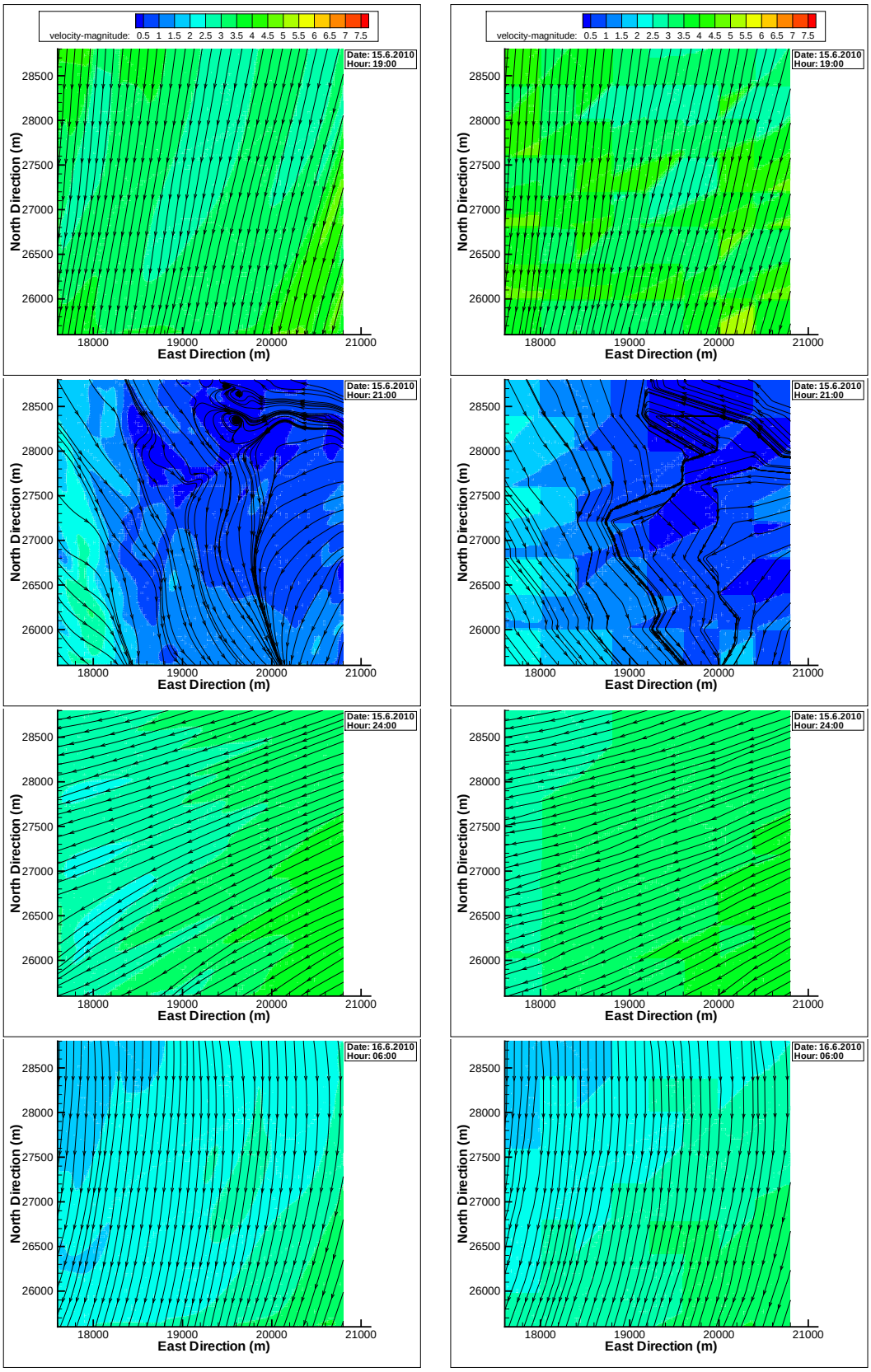


FLUENT Solutions MM5 Solutions

Figure 3.15: Velocity magnitude contours of FLUENT and MM5 solutions 25m above the ground at the 1st, 6th, 12th and 24th hours of the simulation

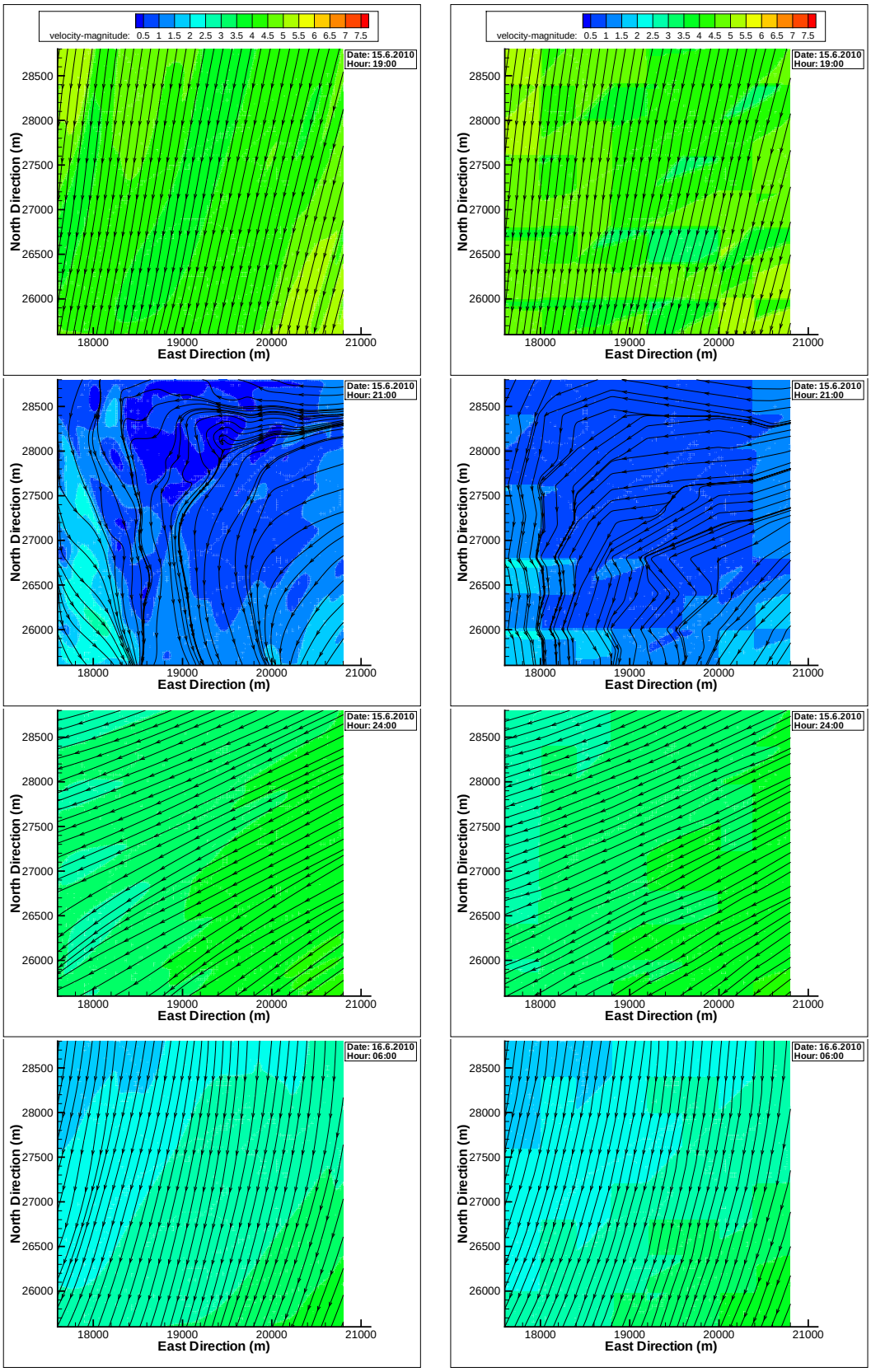


FLUENT Solutions MM5 Solutions

Figure 3.16: Velocity magnitude contours of FLUENT and MM5 solutions 50m above the ground at the 1st, 6th, 12th and 24th hours of the simulation

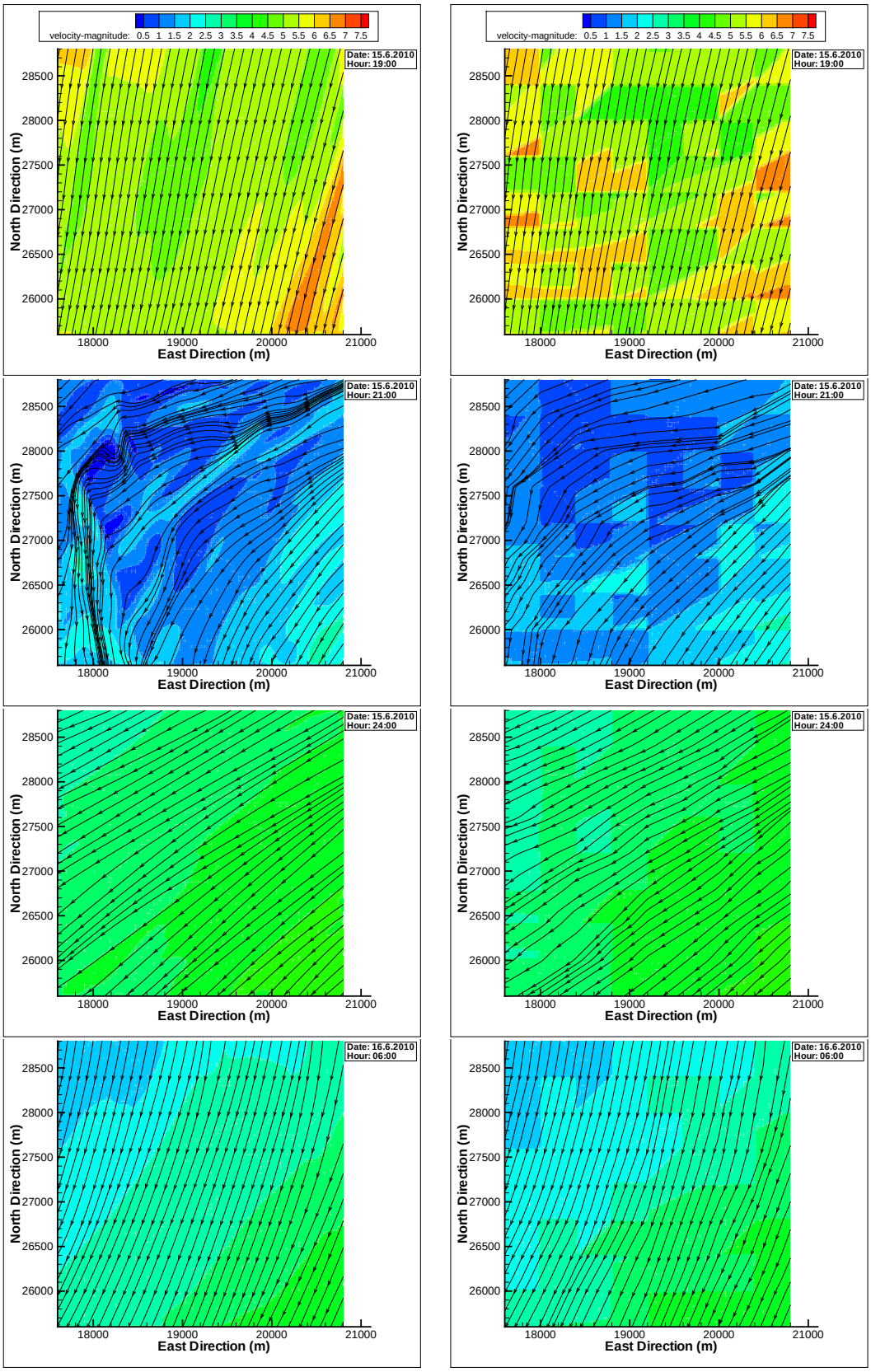


FLUENT Solutions MM5 Solutions

Figure 3.17: Velocity magnitude contours of FLUENT and MM5 solutions 100m above the ground at the 1st, 6th, 12th and 24th hours of the simulation

As seen in Figure 3.15, Figure 3.16 and Figure 3.17; MM5 and FLUENT solutions generally agree well with each other. Because of the low resolution of the MM5 weather prediction data, changes in the velocity magnitudes and wind directions are indicated crudely. The most significant result is observed at the 3rd hour of the simulation. Whereas MM5 fails to capture small disturbances such as swirls, FLUENT solutions represent them quite well.

For further comparison, vectoral velocities of FLUENT and MM5 solutions at the locations of MM5 nodes and their differences are plotted side-by-side after the first hour of the simulation as seen in Figure 3.18. Blue vectors represent the MM5 solution whereas red vectors represent FLUENT solution. Differences between the two solutions are illustrated as purple vectors. As seen in Figure 3.18, difference between the two solutions is bigger near the ground level and gets smaller as altitude is increasing. The reason for these differences is that MM5 doesn't take into account the boundary layer because of the terrain following sigma coordinate assumption.

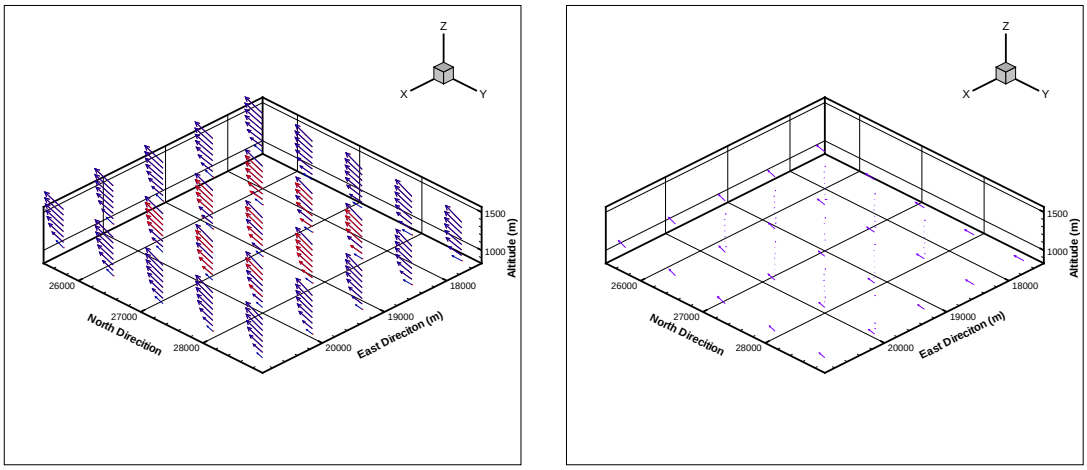


Figure 3.18: Velocity vectors of MM5 and FLUENT solutions and their differences at MM5 node Locations for the 1st hour of the simulation

For better illustration of the differences between MM5, x-velocity and y-velocity components at nodes in the middle of the domain (around Industrial Engineering Department) are plotted along with the values from MM5 at the sixth hour of the simulation as seen in Figure 3.19. Middle of the domain was selected as it is the furthest region

from the boundary conditions thus the effect of MM5 solution data will be minimal.

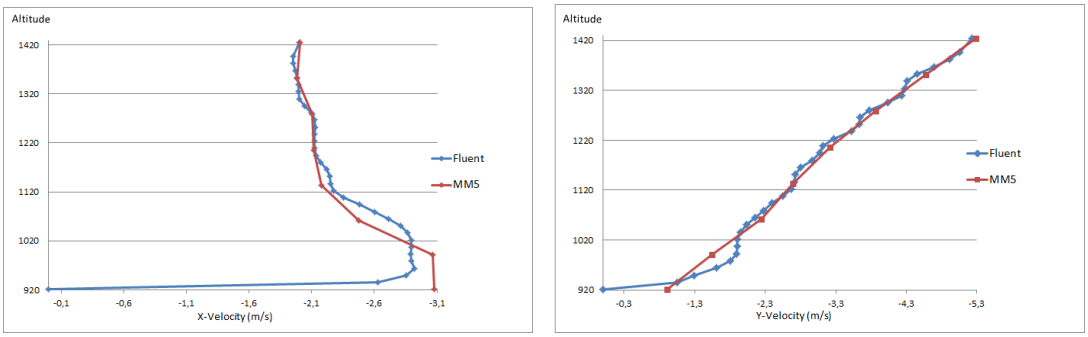


Figure 3.19: X (left) and Y (right) velocities in the middle of the domain for the 6th hour of the simulation

Also, velocity magnitudes at the same locations for the 1st and 12th hours of the simulation are plotted as seen in Figure 3.20, Figure 3.21 and Figure 3.22 respectively.

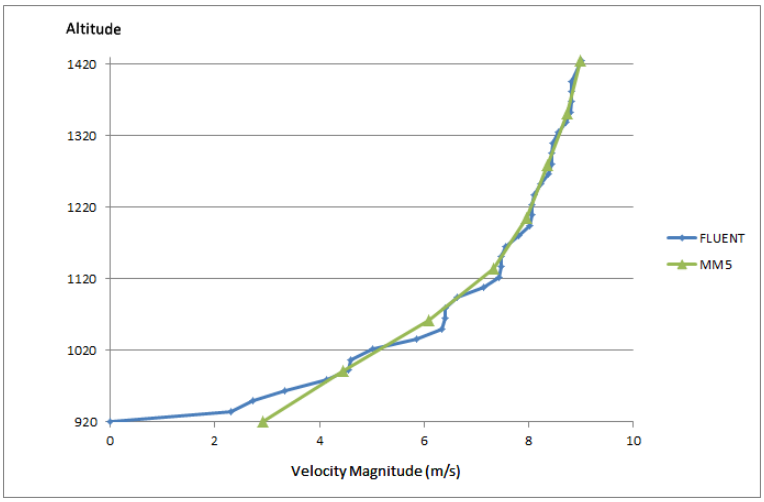


Figure 3.20: Velocity magnitudes of FLUENT and MM5 solutions in the middle of the domain for the 1st hour of the simulation

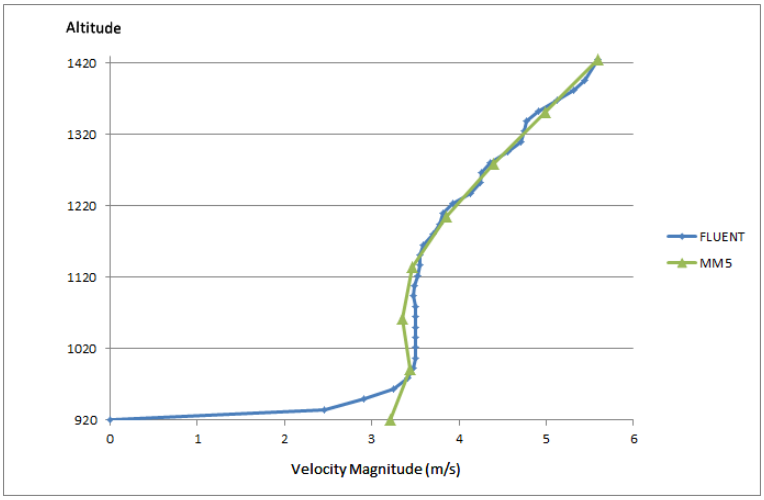


Figure 3.21: Velocity magnitudes of FLUENT and MM5 solutions in the middle of the domain for the 6th hour of the simulation

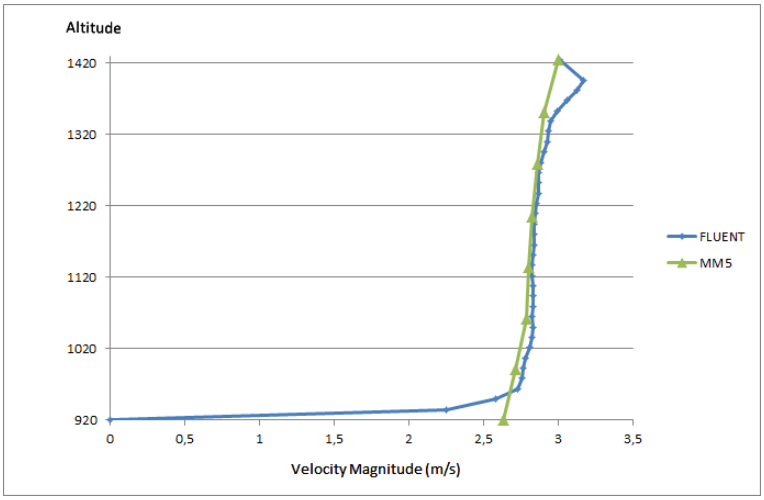


Figure 3.22: Velocity magnitudes of FLUENT and MM5 solutions in the middle of the domain for the 12th hour of the simulation

As seen from Figure 3.20, Figure 3.21 and Figure 3.22, flow in the vicinity of the ground is better resolved and simulated more accurately using the methodology in this study. Oscillations for the FLUENT solutions are thought to occur because of the changes in wind direction.

### 3.1.3 EFFECTS OF SURFACE ROUGHNESS MODEL

As previously mentioned in the Methodology section, surface roughness heights at the MM5 nodes in the FLUENT solution domain can be obtained. Using these roughness height information and Table 2.1, the interface program can generate surface roughness height point profiles for the topography of METU campus as can be seen in Figure 3.23.

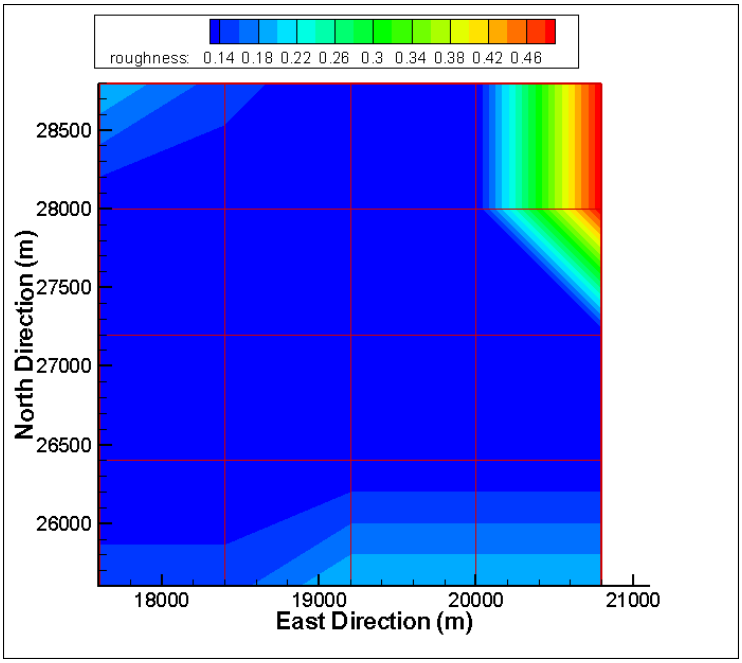


Figure 3.23: Roughness height profile for the topography of METU campus

Hooking this roughness height profile to the topography which is a no-slip wall, FLUENT solutions with roughness profiles are carried out.

For examining the effects of surface roughness height, runs without surface roughness height profiles are performed and velocity magnitude contours with streamlines at the 1st, 6th, 12th and 24th hours of the simulation are plotted with velocity magnitude reduction percent at 25, 50 and 100 meters above the ground in Figure 3.24, Figure 3.25 and Figure 3.26 respectively.

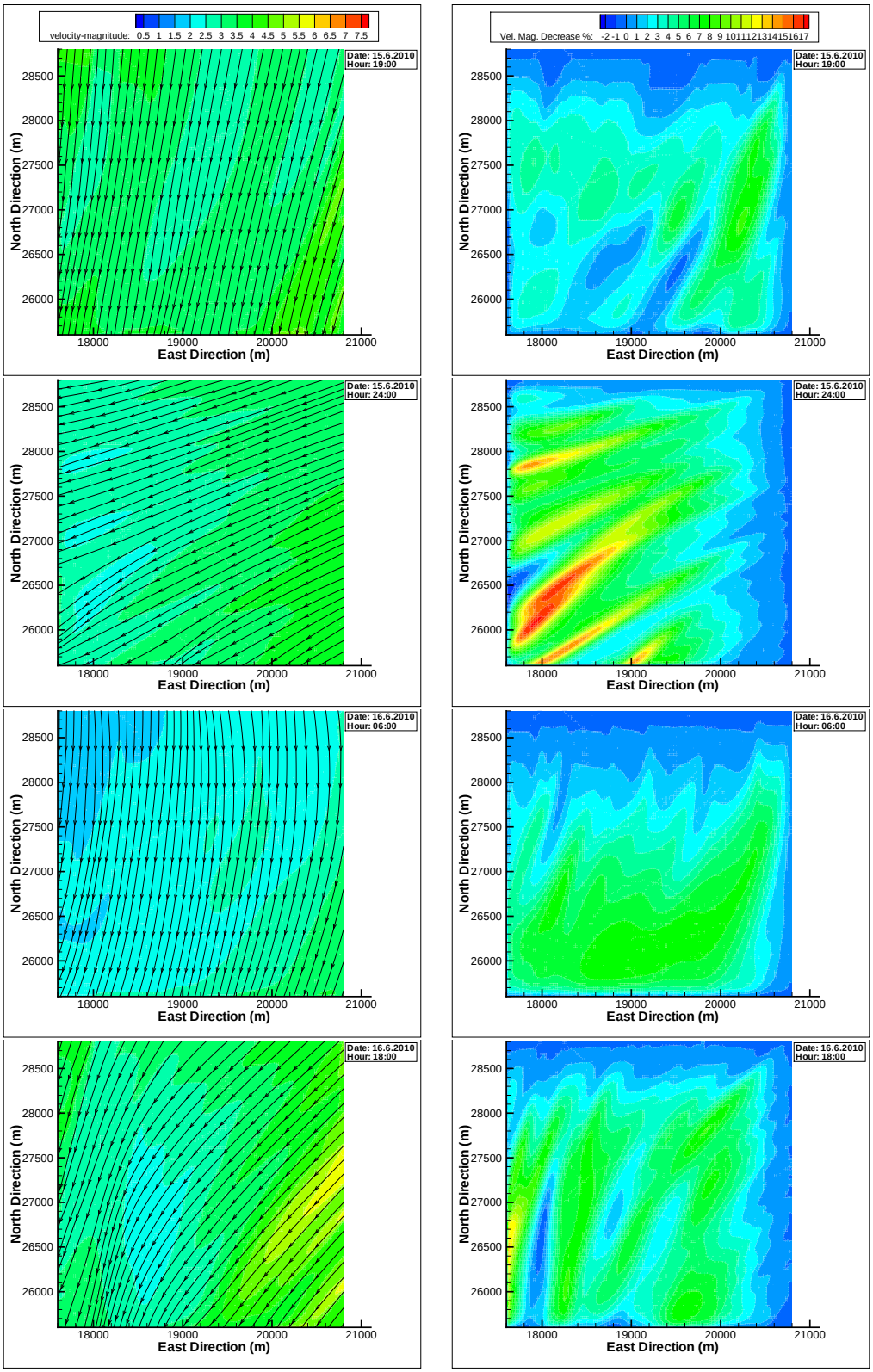


FLUENT solutions with roughness model

Effects of roughness on velocity magnitude

Figure 3.24: Velocity magnitude contours and effects of roughness on velocity magnitude 25m above the ground at the 1st, 6th, 12th and 24th hours of the simulation

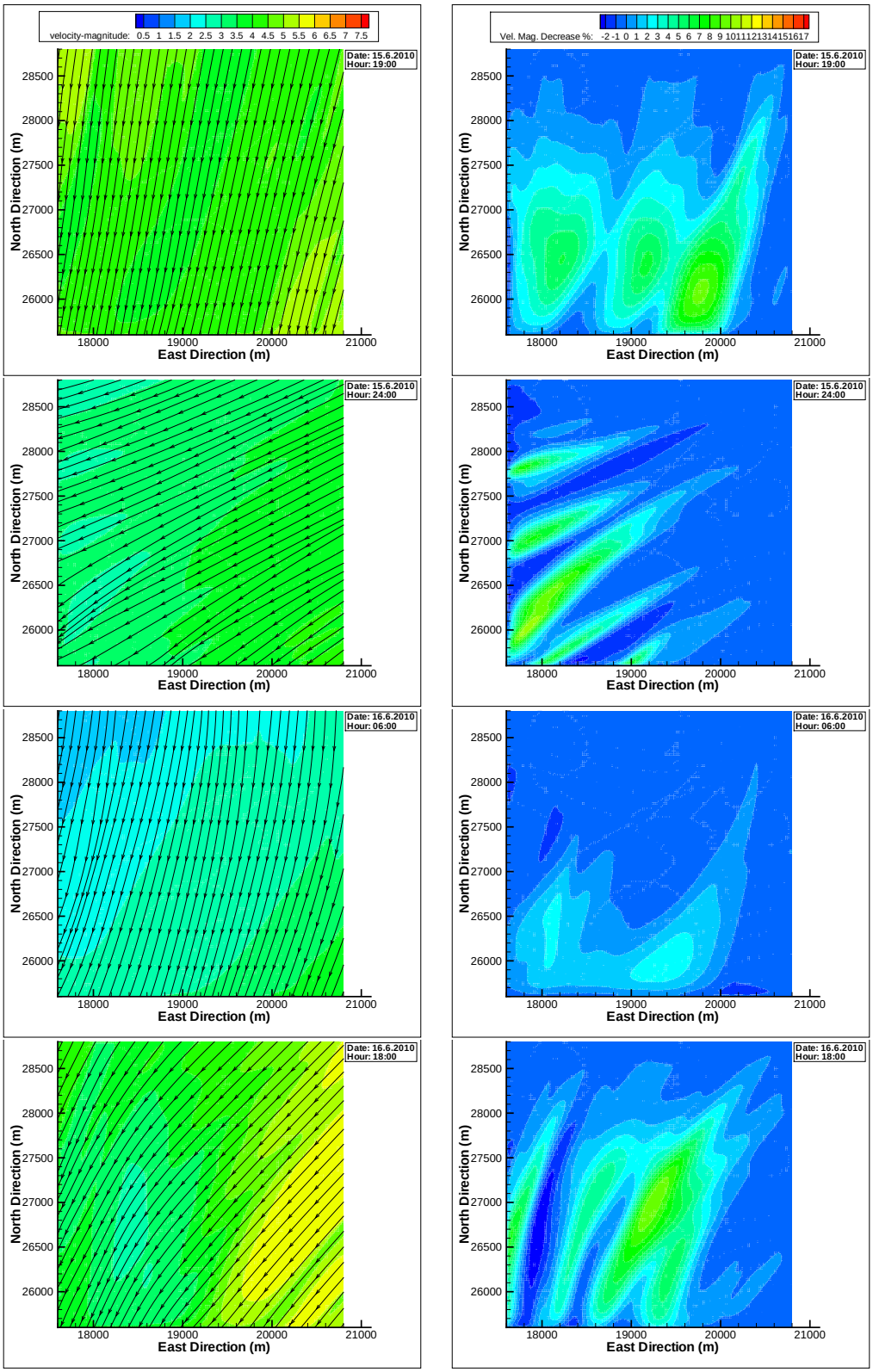


FLUENT solutions with roughness model

Effects of roughness on velocity magnitude

Figure 3.25: Velocity magnitude contours and effects of roughness on velocity magnitude 50m above the ground at the 1st, 6th, 12th and 24th hours of the simulation

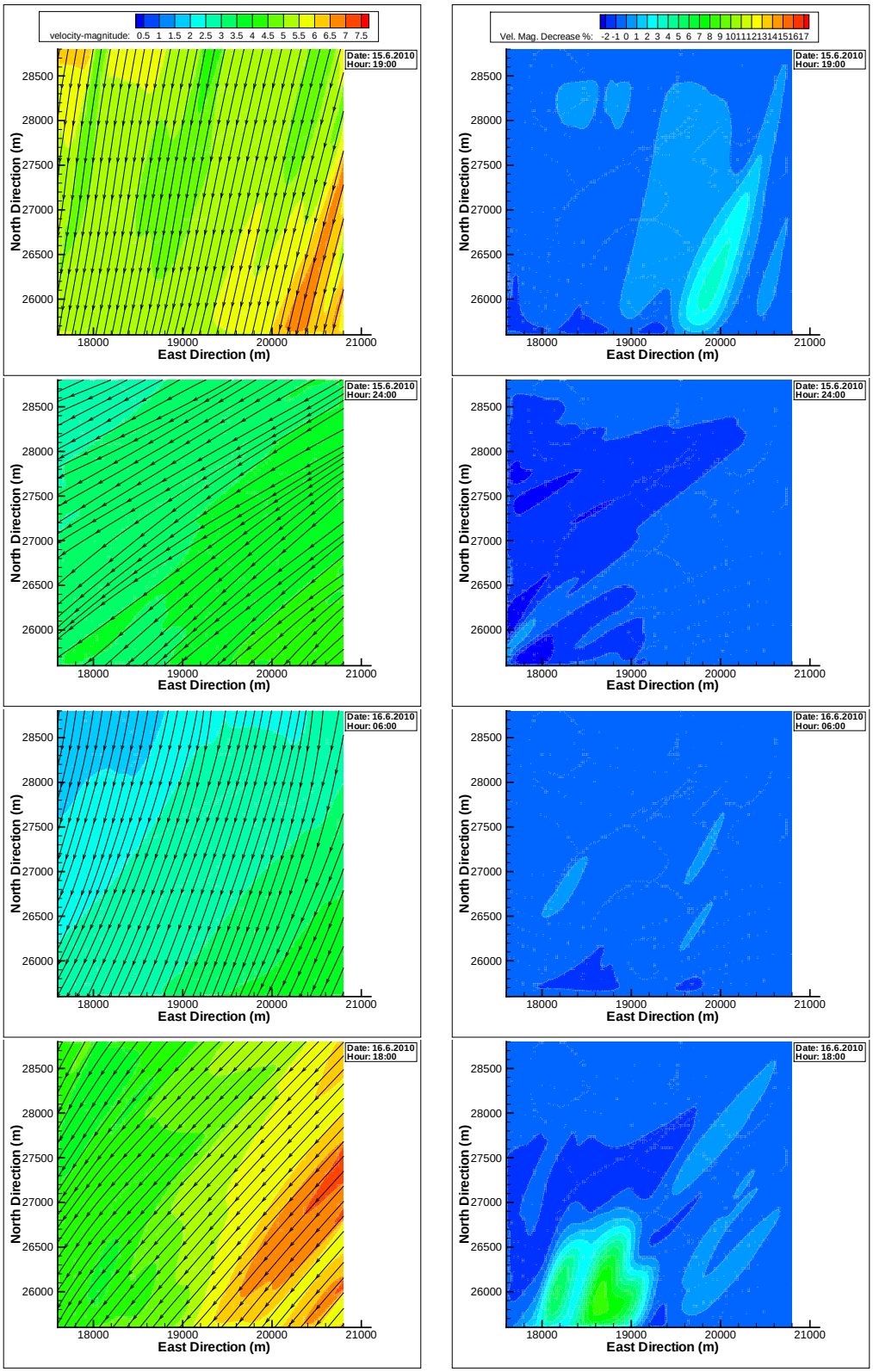


FLUENT solutions with roughness model

Effects of roughness on velocity magnitude

Figure 3.26: Velocity magnitude contours and effects of roughness on velocity magnitude 100m above the ground at the 1st, 6th, 12th and 24th hours of the simulation

As seen in Figure 3.24, Figure 3.25 and Figure 3.26, surface roughness height is important as it can reduce the wind velocity by up to 28 percent near the ground but its effect decays as the altitude gets higher. As the wind power generated is proportional to the third power of the wind velocity, 28 percent reduction in velocity magnitude could give rise to approximately 63 percent reduction of the power. Also; as seen from Figure 3.23 and Figure 3.24, regions which has high velocity magnitude reduction are where the wind passing through high surface roughness length regions exits the domain. It is thought that the effects of high surface heights diffuses and gets bigger as the flow exits the domain.

Moreover; velocity magnitudes in the middle of the domain are presented for the 1st, 6th and 12th hours of the simulation for solutions with and without surface roughness profiles in Figure 3.27, Figure 3.28 and Figure 3.29.

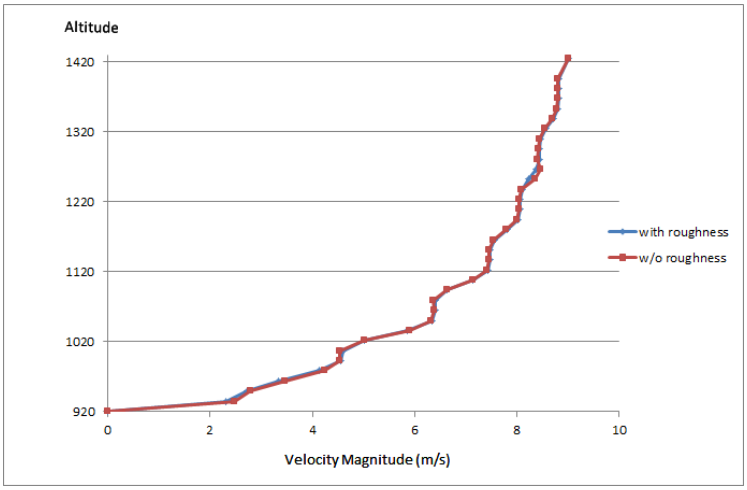


Figure 3.27: Velocity magnitudes with and without roughness height profiles in the middle of the domain for the 1st hour of the simulation

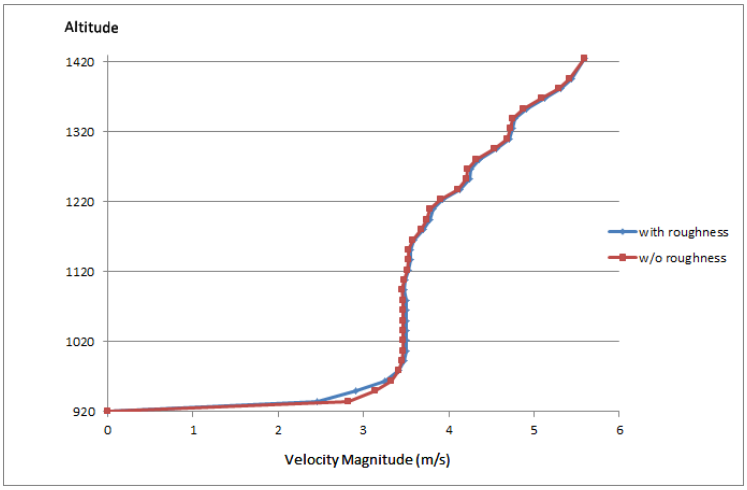


Figure 3.28: Velocity magnitudes with and without roughness height profiles in the middle of the domain for the 6th hour of the simulation

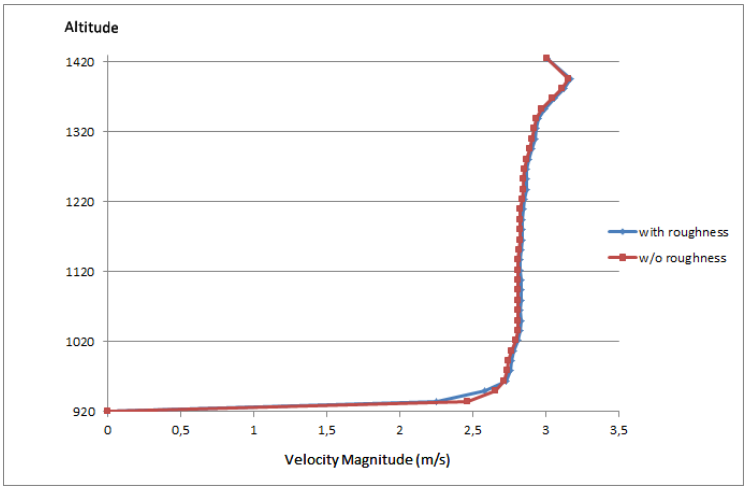


Figure 3.29: Velocity magnitudes with and without roughness height profiles in the middle of the domain for the 12th hour of the simulation

## 3.2 UNSTEADY ATMOSPHERIC FLOW SOLUTIONS OVER TOPOGRAPHICAL TERRAIN WITH HIGH-RISE BUILDING MODELS

Steps for carrying out unsteady atmospheric flow solutions over topographical terrain with high-rise building models are the same as the case without buildings except the discretization of the solution domain. The model of topography should be modified to include high-rise buildings.

For modifying the previously generated flowfield as shown in Figure 3.3; building models are created using locations, orientations and sizes of building models for MM (Mühendislik Merkez Binası) and KKM (Kültür Kongre Merkezi) buildings obtained from Google Earth at the specified x and y locations (east distance, north distance).

Subtracting the building models from the flowfield as previously generated in the case with only topography, a flowfield with building models is generated as seen in Figure 3.30.

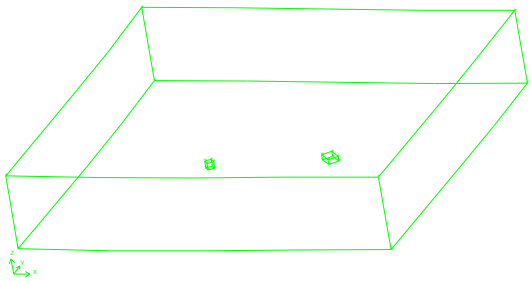

Figure 3.30: Flowfield with high-rise buildings

Firstly, faces of the building models are meshed with 5 meter resolution as seen in Figure 3.31. After that, by generating a size function with growth rate 1.15 and maximum edge length of 80 meters from the lower edges of the buildings to the topography surface mesh is generated as seen in Figure 3.31.

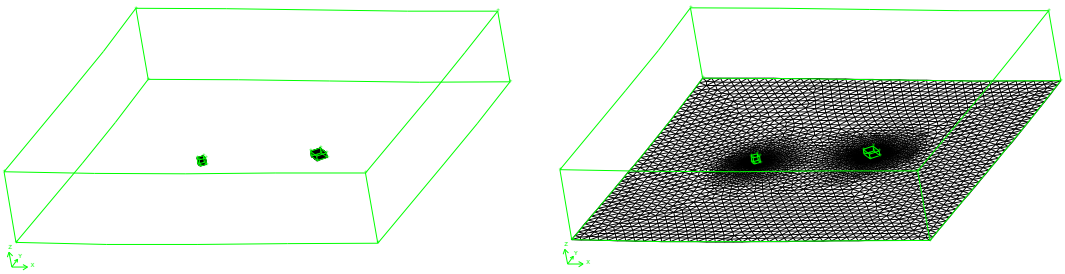

Figure 3.31: Flowfield and meshes on the building models (left) and the surface mesh of the modified topography (right)

Having meshed the topography another size function is generated with a growth rate of 1.15 and maximum edge length of 80 meters from the topography to the 8th sigma level which is the upper bound for the flowfield. Using this size function, an unstructured mesh with 361599 cells is generated for the flowfield as seen in Figure 3.32.

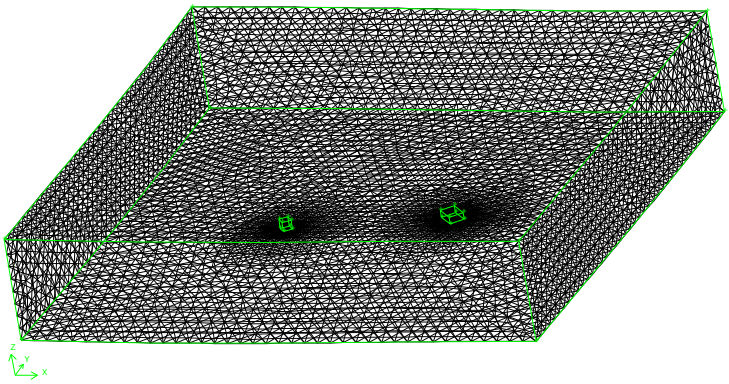

Figure 3.32: Unstructured Mesh of the Flowfield with Building Models

For a more clear illustration x-plane cuts of meshes around building models are presented in Figure 3.33 along with the close-up views around buildings in Figure 3.34.

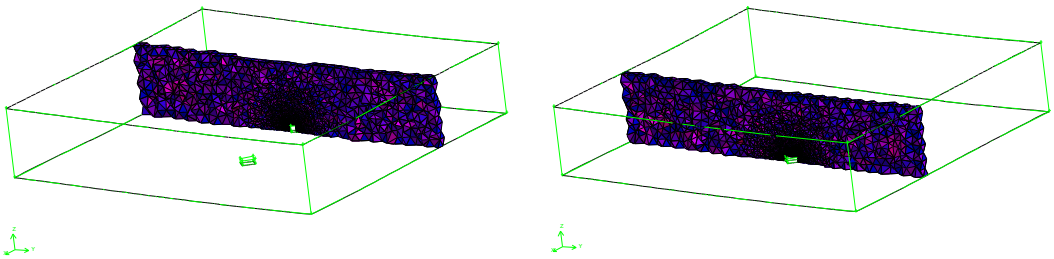

Figure 3.33: X plane cuts of the meshes around building models

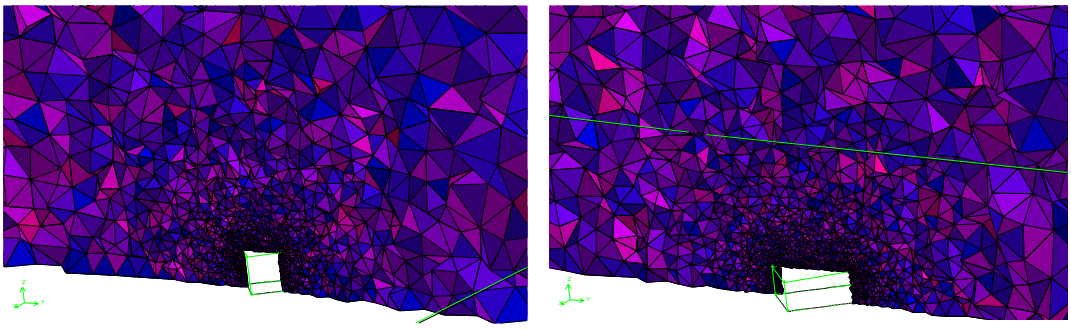

Figure 3.34: Close-up views of the meshes around building models

FLUENT flow solutions over topographical terrain with high-rise building models are observed with z-plane cuts at specific altitudes 960, 985 and 1050 meters, namely as seen in Figure 3.35. Blue, yellow, red colors are used for the surfaces at 960, 985 and 1050 meters of altitudes respectively.

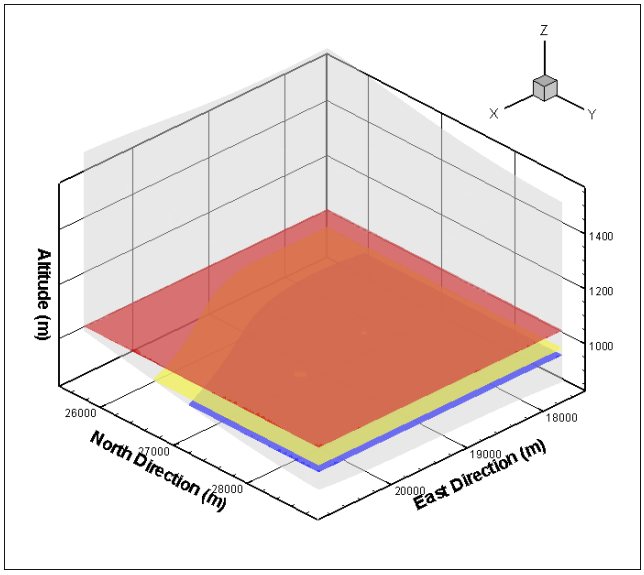


Figure 3.35: FLUENT solution domain with z-plane cuts at 960, 985 and 1050 meters of altitudes

Velocity magnitude contours and streamlines of FLUENT solutions over topographical terrain with building models at the 1st, 6th, 12th and 24th hours of the simulation at 960, 985 and 1050 meters of altitudes are presented in Figure 3.36, Figure 3.37 and Figure 3.38 respectively.

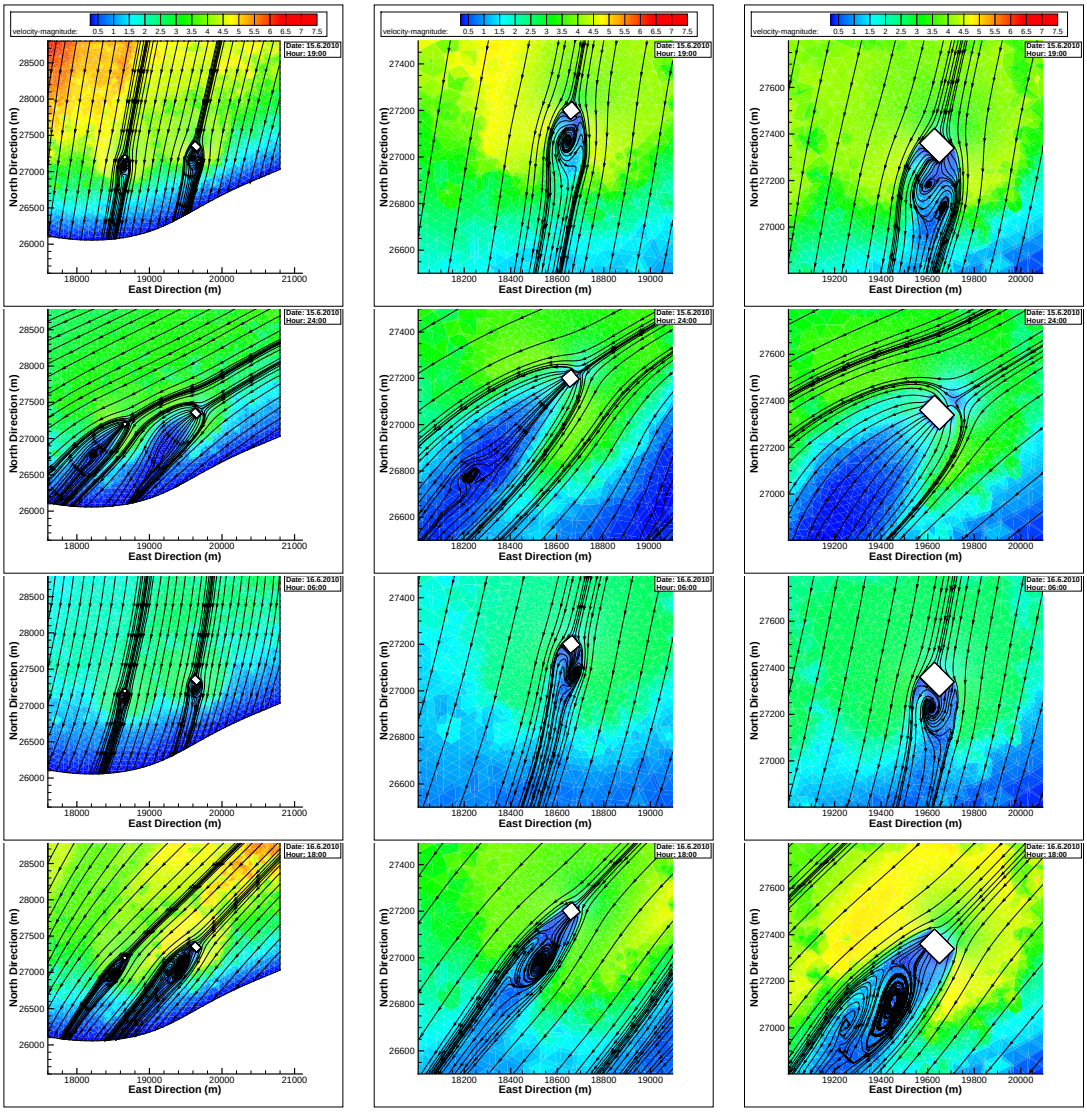


Velocity Contours with Buildings | Close-up View (MM Building) | Close-up View (KKM Building)

Figure 3.36: Velocity Contours and streamlines at 960m altitude at the 1st, 6th, 12th and 24th hour of the Simulation and Close-up Views around MM and KKM Buildings

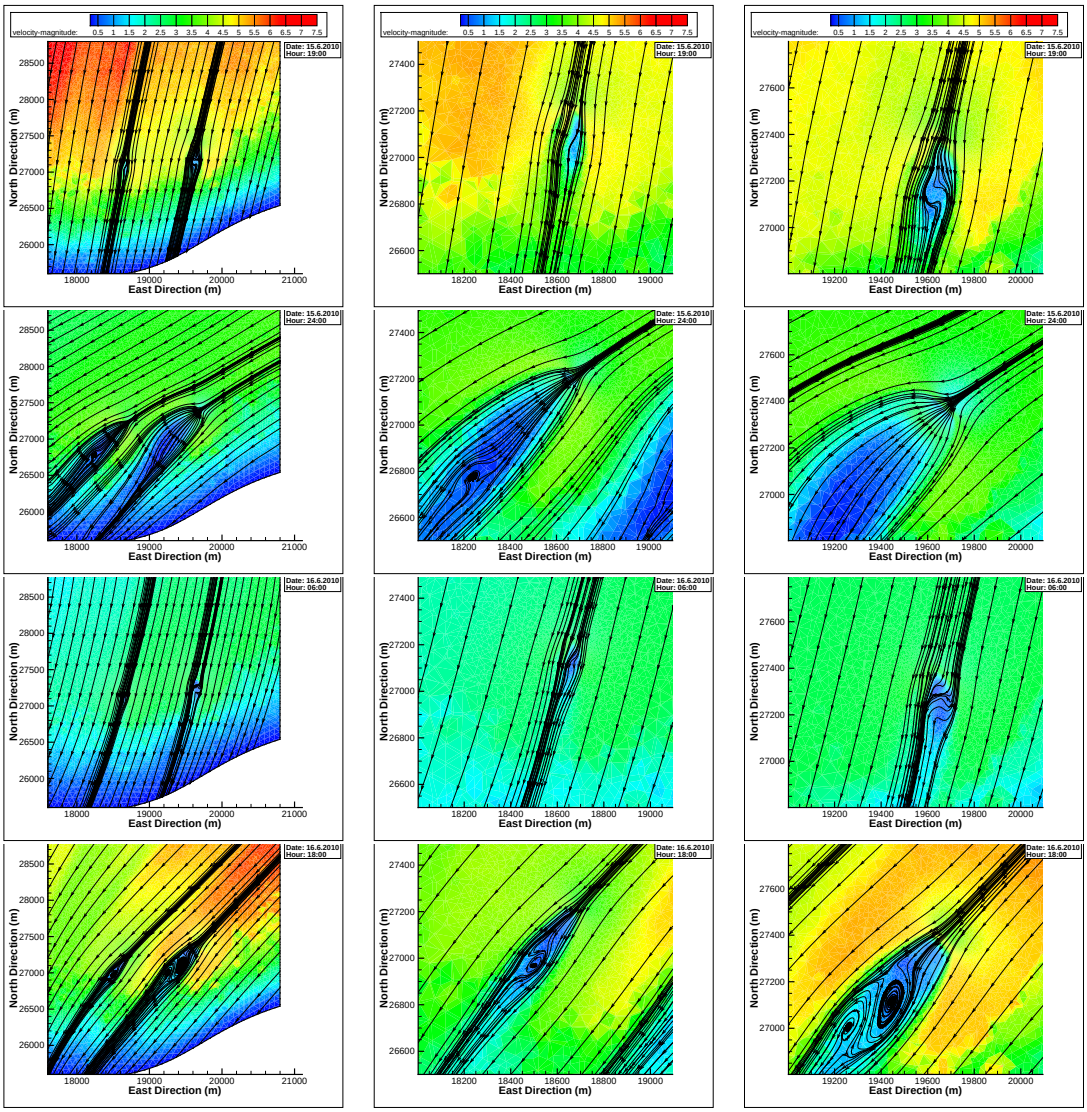


Velocity Contours with Buildings | Close-up View (MM Building) | Close-up View (KKM Building)

Figure 3.37: Velocity Contours and streamlines at 985m altitude at the 1st, 6th, 12th and 24th hour of the Simulation and Close-up Views around MM and KKM Buildings

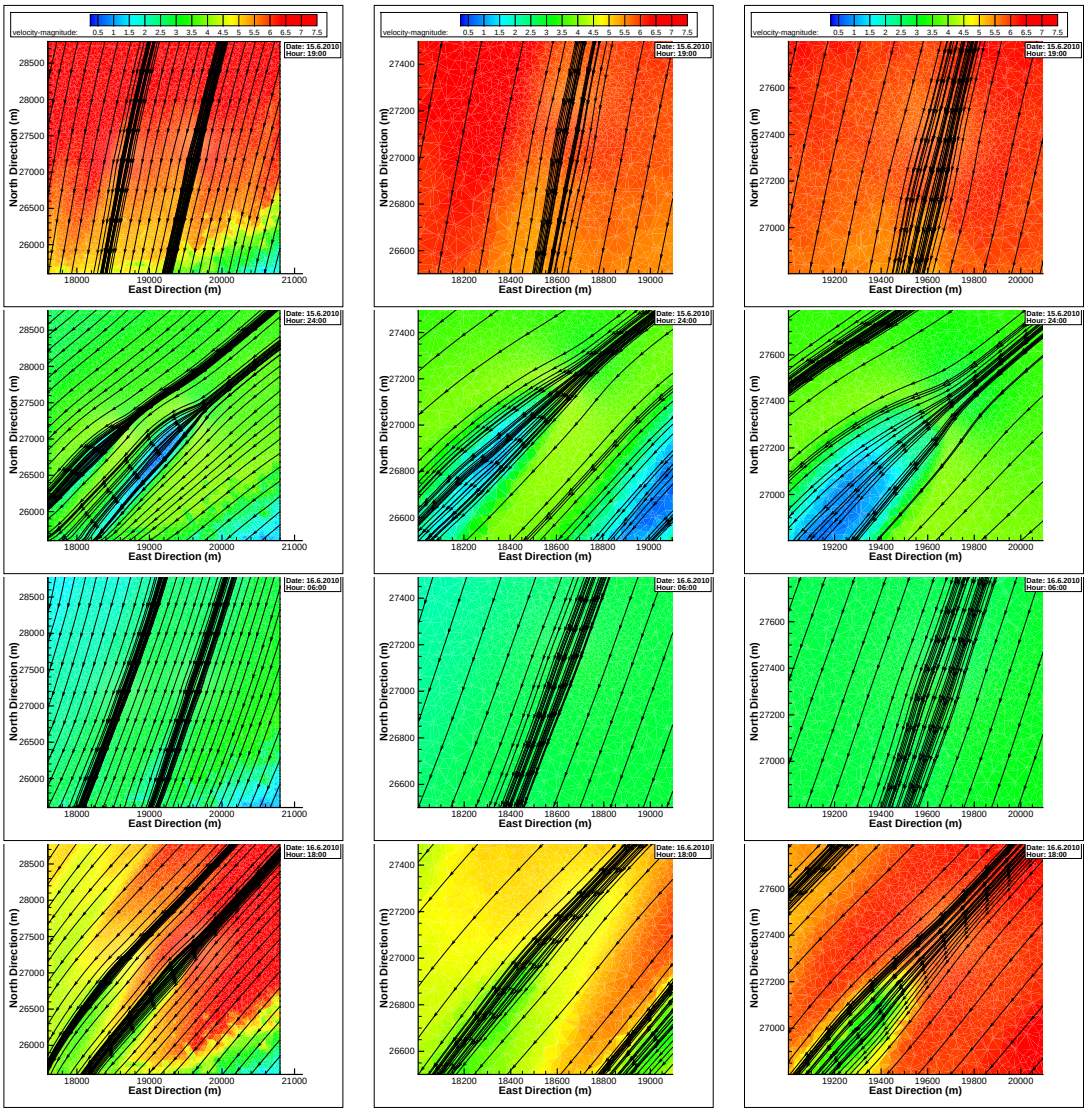


Velocity Contours with Buildings | Close-up View (MM Building) | Close-up View (KKM Building)

Figure 3.38: Velocity Contours and streamlines at 1050m altitude at the 1st, 6th, 12th and 24th hour of the Simulation and Close-up Views around MM and KKM Buildings

As seen in Figure 3.36, Figure 3.37 and Figure 3.38; swirls in the wake of buildings are simulated using unstructured grids which is not available for mesoscale atmospheric weather prediction models. As the resolution for the unstructured mesh is low at regions away from the buildings, contours of velocity magnitude are not satisfying. Moreover it can be seen that the disturbances in the flowfield due to buildings decay as the altitude gets higher.

# CHAPTER 4

# CONCLUSION

In this study, unsteady and turbulent simulations of the atmospheric flows around METU campus are successfully obtained using FLUENT, which is a commercial flow solver, coupled with the MM5 solutions. MM5 is a mesoscale atmospheric weather prediction model and provides the unsteady boundary conditions needed by the unsteady FLUENT solutions. The flow solutions are obtained with and without the building models using unstructured and structured grids respectively. In addition, the surface roughness height profile extracted from the MM5 input data is implemented in the FLUENT solutions successfully.

This coupled solution method developed has the advantage of better resolving the boundary layer flows in the vicinity of the ground surface which is rather important for wind turbine sitings and pollution tracking simulations.

In addition, urban flowfields in the presence highrise buildings are also discretized using unstructured grids. The results obtained show that the presence of highrise buildings significantly disturbs the flowfield and should be considered in the wind turbine siting in the vicinity of urban terrains.

MM5 and FLUENT solutions generally agree well with each other away from the ground surface. In addition, MM5 fails to capture small scale flow features such as swirls while the FLUENT solutions in high resolution, terrain fitted grids represent

them quite well.

Results of this study shows that the wind direction and speed changes rapidly in the vicinity of the ground, extending up to 100m even when observed at 5 minute intervals. Therefore, wind turbine siting studies based on unsteady wind profiles would provide more accurate predictions. Also, it is seen that as the height above the ground increases velocity magnitude increases and irregularities in flowfield tend to decrease. Moreover, velocity magnitudes are higher on elevated surfaces even when observed at the same heights above ground.

Surface roughness height is important as it can reduce the wind velocity by up to 28 percent near the ground but its effect decays as the altitude gets higher. Also; regions which has high velocity magnitude reduction are where the wind passing through high surface roughness height regions exits the domain. It is thought that the effects of high surface heights diffuses and gets bigger as the flow exits the domain.

As a future work, higher order interpolation schemes for the interpolation of MM5 weather forecast data on the computational grid should be developed. In addition, plume dispersion model may also be implemented for pollution tracking studies. Moreover, parallelization of the process can be made to reduce the computational time.

# REFERENCES


[1] Yılmaz, E., quExtreme Wind and Air Quality Modeling/Simulation for a Metropolitan Area, Purdue School of Engineering and Technology, IUPUI, Indianapolis, IN, Presentation, September 2009.

[2] Cochran, B.C., Damiani, R.R., quHarvesting Wind Power from Tall Buildings,WindPower 2008, Houston, Texas June 2-4, June 2008.

[3] Politis, E.S.,Chaviaropoulos, P.K., quMicrositing and classification of wind turbines in complex terrain, 2008 European Wind Energy Conference and Exhibition Brussels, Belgium, March 2008.

[4] Damiani, R., Cochran, B., Orwig, K., Peterka, J., quComplex Terrain: A Valid Wind Option?,American Wind Energy Association, Poster, 2008.

[5] Strangroom, P., quCFD Modelling of Wind Flow Over Terrain, PhD Thesis, The University of Nottingham, January 2004

[6] Derickson R.G., Peterka J.A. quDevelopment of a Powerful Hybrid Tool for Evaluating Wind Power in Complex Terrain: Atmospheric Numerical Models and Wind Tunnels, American Institute of Aeronautics and Astronautics, 2004.

[7] P.S. Jackson and J.C.R. Hunt, quTurbulent wind flow over a low hill, Q. J. Roy. Meteorol. Soc. 101, p. 929-955, 1975.

[8] N. G. Mortensen, D. N. Heathfield, L. Myllerup, L. Landberg and O. Rathmann, quGetting Started with WAsP 9, Risø National Laboratory, Roskilde, Denmark, June 2007.

[9] D. Heinemann, Wind Flow Modelling - The Bases for Resource Assessment and Wind Power Forecasting, Presentation, ForWind Center for Wind Energy Research Energy Meteorology Unit, Oldenburg University.

[10] Anthony J. Bowen nad Niels G. Mortensen, quWAsP prediction errors due to site orography, Risø National Laboratory, Roskilde, Denmark, December 2004

[11] Botta, G., Castagna, R., Borghetti, M. and Mantegna, D. , qu Wind analysis on complex terrain - The case of Acqua Spruzza, Jour. Wind Eng. Ind. Aerodyn. 39, 357-66., 1992.

[12] Bowen, A.J. and Saba, T., quThe evaluation of software for wind turbine siting in hilly terrain, Proc. 9th International Conference on Wind Engineering, New Delhi, India, January 1995.

[13] Reid, S.J., quModelling of channelled winds., Proc. BWEA Conference, Warwick, UK, 391-6, July 1995.

[14] Sempreviva, A.M., Troen, I. and Lavagnini, A., Modelling of wind power potential in Sardinia. Proc. European Wind Energy Association Conference and Exhibition, Rome Italy, October 1986.

[15] Lindley, D., Musgrove, P., Warren, J. and Hoskin, R., quOperating experience from four UK wind farms. Proc. 15th BWEA Annual Wind Energy Conference, York, UK, 41-45, October 1993.

[16] Frank J.Zajaczkowski, SueEllenHaupt, KerrieJ.Schmehl, quA preliminary study of assimilating numerical weather prediction data into computational fluid dynamics models for wind prediction, Journal of Wind Engineering and Industrial Aerodynamics, 99, 320-329, March 2011.

[17] M.H. Zheng, Y.R. Guo, X.Q. Ai, T. Qin, quCoupling GIS with CFD Modeling to Simulate Urban Pollutant Dispersion, Mechanic Automation and Control Engineering (MACE), 2010 International Conference Wuhan China, June 2010.

[18] Laurent Laporte, Éric Dupont,Bertrand Carissimo, Luc Musson-Genon, Cyril Sécolier, quAtmospheric CFD Simulations coupled to Mesoscale Analyses for Wind Resource assessment in complex terrain, European Wind Energy Conference and Exhibition (EWEC)/Marseille, France, March 2009

[19] Mesoscale and Microscale Meteorology Division, National Center for Atmospheric Research, quPSU/NCAR Mesoscale Modeling System Tutorial Class Notes and User's Guide, NCAR, Penn State, January 2005.

[20] T.R. Oke, Boundary Layer Climates Cambridge: University Press, 1987.

[21] GAMBIT 2.4.6 User Manual FLUENT Inc. , 2007

[22] FLUENT 6.3.26 User Guide FLUENT Inc. , 2006

[23] Patankar, S. V. and Spalding, D.B., A calculation procedure for heat, mass and momentum transfer in three-dimensional parabolic flows, Int. J. of Heat and Mass Transfer, Volume 15, Issue 10, Pages 1787-1806, October 1972.

[24] Mortensen, N.G., Hansen, J.C., Badger, J., Jorgensen, B.H., Hasager, C.B., Paulsen, U.S., Hansen, O.F., Enevoldsen K., Youssef, L.G., Said, U.S., Moussa, A.A.E., Mahmoud, M.A., Yousef, A.E.S., Awad, A.M., Ahmed, M.A.R., Sayed, M.A.M., Korany, M.H., M.A.B.T Tarad, Wind Atlas For Egypt: Measurements, Micro-And Mesoscale Modelling,Proceedings of the 2006 European Wind Energy Conference and Exhibition, Athens, Greece, February 27 to March 2. 10 pp., March 2006